performed using vervet monkeys and rhesus macaques. Male vervet monkeys with a high rank within a group's social dominance hierarchy demonstrate elevated levels of serotonin in the blood and higher levels of the serotonin metabolite 5-hydroxyindoleacetic acid (5-HIAA) in the cerebrospinal fluid (CSF) [21]. When drugs that increase serotonin transmission were administered to an individual, they acquired a higher dominance status in the colony [25]. Conversely, low CSF 5-HIAA levels were associated with increased ratings of aggression and risk-taking behavior in adolescent male rhesus macaques [19,20]. It is unclear, however, how measurements of whole blood 5-HT or CSF levels of 5-HIAA that relate to the actual functional turnover of 5-HT in discrete regions of the brain are associated with social behavior [17]. Our results might present a potential molecular mechanism for the elevated biosynthesis of 5HTP function in chimpanzee dominance-related behavioral traits.

To elucidate the total neurochemical mechanism for serotonin function, we may also need to conduct a survey on the other serotonin-related genes. Among such genes, tandem repeat polymorphisms in the 5′ promoter regions of serotonin transporter (5HTT) or monoamine oxidase A (MAOA) genes, which are associated with personality traits in humans, have been surveyed in chimpanzees and have shown less or low frequencies polymorphism [12,13]. Therefore, the TPH2 polymorphism reported in this study is particularly important in individual differences in the behaviors among chimpanzees. In future studies, detection of the levels of 5-HIAA in CSF in chimpanzees may facilitate the understanding total serotonin function in the brain. Also, we are searching polymorphic markers relating several serotonin receptor genes in chimpanzees.

Acknowledgement

We are indebted to the late Professor O. Takenaka, Primate Research Institute, Kyoto Univerisy, for providing the primate samples.

References

[1] A.J. Bennett, K.P. Lesch, A. Heils, J.C. Long, J.G. Lorenz, S.E. Shoaf, M. Champoux, S.J. Suomi, M.V. Linnoila, J.D. Higley, Early experience and serotonin transporter gene variation interact to influence primate CNS function, Mol. Psychiatry 7 (2002) 118–122.

[2] L. Cervo, A. Canetta, E. Calcagno, S. Burbassi, G. Sacchetti, S. Caccia, C. Fracasso, D. Albani, G. Forloni, R.W. Invernizzi, Genotype-dependent activity of tryptophan hydroxylase-2 determines the response to citalopram in a mouse model of depression, J. Neurosci. 25 (2005) 8165–8172.

[3] G.L. Chen, M.A. Novak, S. Hakim, Z. Xie, G.M. Miller, Tryptophan hydroxylase-2 gene polymorphisms in rhesus monkeys: association with hypothalamic-pituitary-adrenal axis function and *in vitro* gene expression, Mol. Psychiatry 11 (2006) 914–928.

[4] F. Côté, E. Thévenot, C. Fligny, Y. Fromes, M. Darmon, M.A. Ripoche, E. Bayard, N. Hanoun, F. Saurini, P. Lechat, L. Dandolo, M. Hamon, J. Mallet, G. Vodjdani, Disruption of the nonneuronal tph1 gene demonstrates the importance of peripheral serotonin in cardiac function, Proc. Natl. Acad. Sci. USA 100 (2003) 13525–13530.

[5] V. De Luca, D.J. Mueller, S. Tharmalingam, N. King, J.L. Kennedy, Analysis of the novel TPH2 gene in bipolar disorder and suicidality, Mol. Psychiatry 9 (2004) 896–897.

[6] H. Erlandsen, F. Fusetti, A. Martinez, E. Hough, T. Flatmark, R.C. Stevens, Crystal structure of the catalytic domain of human phenylalanine hydroxylase reveals the structural basis for phenylketonuria, Nat. Struct. Biol. 4 (1997) 995–1000.

[7] K.E. Goodwill, C. Sabatier, C. Marks, R. Raag, P.F. Fitzpatrick, R.C. Stevens, Crystal structure of tyrosine hydroxylase at 2.3 A and its implications for inherited neurodegenerative diseases, Nat. Struct. Biol. 4 (1997) 578–585.

[8] H.E. Grenett, F.D. Ledley, L.L. Reed, S.L. Woo, Full-length cDNA for rabbit tryptophan hydroxylase: functional domains and evolution of aromatic amino acid hydroxylases, Proc. Natl. Acad. Sci. USA 84 (1987) 5530–5534.

[9] M. Harvey, E. Shink, M. Tremblay, B. Gagne, C. Raymond, M. Labbe, D.J. Walther, M. Bader, N. Barden, Support for the involvement of TPH2 gene in affective disorders, Mol. Psychiatry 9 (2004) 980–981.

[10] H. Hasegawa, A. Ichiyama, Tryptophan 5-monooxygenase from mouse mastocytoma: high-performance liquid chromatography assay, Methods Enzymol. 142 (1987) 88–92.

[11] Y. Iida, K. Sawabe, M. Kojima, K. Oguro, N. Nakanishi, H. Hasegawa, Proteasome-driven turnover of tryptophan hydroxylase is triggered by phosphorylation in RBL2H3 cells, a serotonin producing mast cell line, Eur. J. Biochem. 269 (2002) 4780–4788.

[12] M. Inoue-Murayama, N. Mishima, I. Hayasaka, S. Ito, Y. Murayama, Divergence of ape and human monoamine oxidase A gene promoters: comparative analysis of polymorphisms, tandem repeat structures and transcriptional activities on reporter gene expression, Neurosci. Lett. 405 (2006) 207–211.

[13] M. Inoue-Murayama, Y. Niimi, O. Takenaka, Y. Murayama, Evolution of personality-related genes in primates, in: K. Miyoshi, C.M. Shapiro, M. Gaviria, Y. Morita (Eds.), Contemporary Neuropsychiatry, Springer, Tokyo, 2001, pp. 425–428.

[14] S. Kaufman, New tetrahydrobiopterin-dependent systems, Annu. Rev. Nutr. 13 (1993) 261–286.

[15] L. Kruglyak, D.A. Nickerson, Variation is the spice of life, Nat. Genet. 27 (2001) 234–236.

[16] A.V. Kulikov, D.V. Osipova, V.S. Naumenko, N.K. Popova, Association between Tph2 gene polymorphism, brain tryptophan hydroxylase activity and aggressiveness in mouse strains, Genes Brain Behav. 4 (2005) 482–485.

[17] I. Lucki, The spectrum of behaviors influenced by serotonin, Biol. Psychiatry 44 (1998) 151–162.

[18] I. Lucki, A. Dalvi, A.J. Mayorga, Sensitivity to the effects of pharmacologically selective antidepressants in different strains of mice, Psychopharmacology (Berl.) 155 (2001) 315–322.

[19] J. McKinney, P.M. Knappskog, J. Haavik, Different properties of the central and peripheral forms of human tryptophan hydroxylase, J. Neurochem. 92 (2005) 311–320.

[20] P.T. Mehlman, J.D. Higley, I. Faucher, A.A. Lilly, D.M. Taub, J. Vickers, S.J. Suomi, M. Linnoila, Low CSF 5-HIAA concentrations and severe aggression and impaired impulse control in nonhuman primates, Am. J. Psychiatry 151 (1994) 1485–1491.

[21] P.T. Mehlman, J.D. Higley, B.J. Fernald, F.R. Sallee, S.J. Suomi, M. Linnoila, CSF 5-HIAA, testosterone, and sociosexual behaviors in free-ranging male rhesus macaques in the mating season, Psychiatry Res. 72 (1997) 89–102.

[22] T.K. Newman, Y.V. Syagailo, C.S. Barr, J.R. Wendland, M. Champoux, M. Graessle, S.J. Suomi, J.D. Higley, K.P. Lesch, Monoamine oxidase A gene promoter variation and rearing experience influences aggressive behavior in rhesus monkeys, Biol. Psychiatry 57 (2005) 167–172.

[23] P.D. Patel, C. Pontrello, S. Burke, Robust and tissue-specific expression of TPH2 versus TPH1 in rat raphe and pineal gland, Biol. Psychiatry 55 (2004) 428–433.

[24] E.J. Peters, S.L. Slager, P.J. McGrath, J.A. Knowles, S.P. Hamilton, Investigation of serotonin-related genes in antidepressant response, Mol. Psychiatry 9 (2004) 879–889.

[25] M.J. Raleigh, M.T. McGuire, G.L. Brammer, D.B. Pollack, A. Yuwiler, Serotonergic mechanisms promote dominance acquisition in adult male vervet monkeys, Brain Res. 559 (1991) 181–190.

[26] S.A. Sakowski, T.J. Geddes, D.M. Kuhn, Mouse tryptophan hydroxylase isoform 2 and the role of proline 447 in enzyme function, J. Neurochem. 96 (2006) 758–765.
[27] K.B. Thomas, A.D. Brown, P.M. Iuvone, Elevation of melatonin in chicken retina by 5-hydroxytryptophan: differential light/dark responses, Neuroreport 9 (1998) 4041–4044.
[28] D.J. Walther, J.U. Peter, S. Bashammakh, H. Hortnagl, M. Voits, H. Fink, M. Bader, Synthesis of serotonin by a second tryptophan hydroxylase isoform, Science 299 (2003) 76.
[29] G.J. Yohrling 4th, S.M. Mockus, K.E. Vrana, Identification of amino-terminal sequences contributing to tryptophan hydroxylase tetramer formation, J. Mol. Neurosci. 12 (1999) 23–34.
[30] G.J. Yohrling 4th, G.C. Jiang, S.M. Mockus, K.E. Vrana, Intersubunit binding domains within tyrosine hydroxylase and tryptophan hydroxylase, J. Neurosci. Res. 61 (2000) 313–320.
[31] X. Zhang, J.M. Beaulieu, T.D. Sotnikova, R.R. Gainetdinov, M.G. Caron, Tryptophan hydroxylase-2 controls brain serotonin synthesis, Science 305 (2004) 217.
[32] X. Zhang, R.R. Gainetdinov, J.M. Beaulieu, T.D. Sotnikova, L.H. Burch, R.B. Williams, D.A. Schwartz, K.R. Krishnan, M.G. Caron, Loss-of-function mutation in tryptophan hydroxylase-2 identified in unipolar major depression, Neuron 45 (2005) 11–16.
[33] X. Zhang, J.M. Beaulieu, R.R. Gainetdinov, M.G. Caron, Functional polymorphisms of the brain serotonin synthesizing enzyme tryptophan hydroxylase-2, Cell. Mol. Life Sci. 63 (2006) 6–11.
[34] P. Zill, T.C. Baghai, P. Zwanzger, C. Schule, D. Eser, R. Rupprecht, H.J. Moller, B. Bondy, M. Ackenheil, SNP and haplotype analysis of a novel tryptophan hydroxylase isoform (TPH2) gene provide evidence for association with major depression, Mol. Psychiatry 9 (2004) 1030–1036.

Human Molecular Genetics, 2007, Vol. 16, No. 1 15–23
doi:10.1093/hmg/ddl437
Advance Access published on November 29, 2006

The *DYRK1A* gene, encoded in chromosome 21 Down syndrome critical region, bridges between β-amyloid production and tau phosphorylation in Alzheimer disease

Ryo Kimura[1,†], Kouzin Kamino[1,*,†], Mitsuko Yamamoto[1], Aidaralieva Nuripa[1], Tomoyuki Kida[1], Hiroaki Kazui[1], Ryota Hashimoto[1], Toshihisa Tanaka[1], Takashi Kudo[1], Hidehisa Yamagata[2], Yasuharu Tabara[3], Tetsuro Miki[4], Hiroyasu Akatsu[5], Kenji Kosaka[5], Eishi Funakoshi[6], Kouhei Nishitomi[7], Gaku Sakaguchi[7], Akira Kato[7], Hideyuki Hattori[8], Takeshi Uema[9] and Masatoshi Takeda[1]

[1]Department of Psychiatry, Osaka University Graduate School of Medicine, 2-2-D3 Yamadaoka, Suita, Osaka 565-0871, Japan, [2]Department of Preventive Medicine, [3]Department of Basic Medical Research and Education and [4]Department of Geriatric Medicine, Ehime University Graduate School of Medicine, Toon, Ehime, Japan, [5]Choju Medical Institute, Fukushimura Hospital, Toyohashi, Aichi, Japan, [6]Department of Biochemistry, Faculty of Pharmaceutical Sciences, Setsunan University, Hirakata, Osaka, Japan, [7]Pain and Neurology, Discovery Research Laboratories, Shionogi & Co., Ltd, Shiga, Japan, [8]Department of Psychiatry, Chubu National Hospital, Ohbu, Japan and [9]Department of Psychiatry, Osaka General Medical Center, Osaka, Japan

Received September 7, 2006; Revised and Accepted November 13, 2006

We scanned throughout chromosome 21 to assess genetic associations with late-onset Alzheimer disease (AD) using 374 Japanese patients and 375 population-based controls, because trisomy 21 is known to be associated with early deposition of β-amyloid (Aβ) in the brain. Among 417 markers spanning 33 Mb, 22 markers showed associations with either the allele or the genotype frequency ($P < 0.05$). Logistic regression analysis with age, sex and apolipoprotein E (*APOE*)-ε4 dose supported genetic risk of 17 markers, of which eight markers were linked to the *SAMSN1*, *PRSS7*, *NCAM2*, *RUNX1*, *DYRK1A* and *KCNJ6* genes. In logistic regression, the *DYRK1A* (dual-specificity tyrosine-regulated kinase 1A) gene, located in the Down syndrome critical region, showed the highest significance [OR = 2.99 (95% CI: 1.72–5.19), $P = 0.001$], whereas the *RUNX1* gene showed a high odds ratio [OR = 23.3 (95% CI: 2.76–196.5), $P = 0.038$]. *DYRK1A* mRNA level in the hippocampus was significantly elevated in patients with AD when compared with pathological controls ($P < 0.01$). *DYRK1A* mRNA level was upregulated along with an increase in the Aβ-level in the brain of transgenic mice, overproducing Aβ at 9 months of age. In neuroblastoma cells, Aβ induced an increase in the *DYRK1A* transcript, which also led to tau phosphorylation at Thr^{212} under the overexpression of tau. Therefore, the upregulation of *DYRK1A* transcription results from Aβ loading, further leading to tau phosphorylation. Our result indicates that DYRK1A could be a key molecule bridging between β-amyloid production and tau phosphorylation in AD.

*To whom correspondence should be addressed. Tel: +81 668793051; Fax: +81 668793059; Email: kkamino@psy.med.osaka-u.ac.jp
†The authors wish it to be known that, in their opinion, the first two authors should be regarded as joint First Authors.

INTRODUCTION

Alzheimer disease (AD) is the major cause of dementia in the elderly and is pathologically characterized by senile plaques with β-amyloid deposition (Aβ) and neurofibrillary tangles harboring hyperphosphorylated tau in the brain. It is well established that familial autosomal-dominant early onset AD is mostly caused by mutations of the amyloid protein precursor (*APP*) and presenilin 1 and 2 (*PS1* and *PS2*) genes (1). In contrast, Down syndrome (DS) is also highlighted as a model condition predisposing to AD, because patients with DS develop early deposition of Aβ in the brain (2). Therefore, it has been speculated that genetic factors related to AD could exist on chromosome 21, independent of the ε4 allele of the apolipoprotein E gene (*APOE*-ε4), a known strong risk for late-onset AD (3,4). Using the candidate approach, it was reported that duplication of the *APP* gene was transmitted in patients with familial autosomal-dominant early onset AD with cerebral angiopathy (5), whereas an association with the *APP* gene, to the best of our knowledge, was not supported in case–control studies (6–8). The *BACE2* gene, encoding β-secretase of APP, was not associated with AD; however, recent studies showed weak associations (9–11). In contrast, with the positional approach, genome scans of late-onset AD showed positive linkage on chromosome 21 (12,13). Although this linkage remains controversial (14–16), a locus strongly influencing age at onset was also found on chromosome 21 (17). To search for genetic factors for late-onset AD on chromosome 21, we scanned throughout this chromosome using patients with Japanese late-onset AD and population-based controls, by a stepwise single nucleotide polymorphism (SNP) scan. We report that the *DYRK1A* gene is a genetic factor related to the progression of AD.

RESULTS

Chromosome 21 scan

An exploratory scan of chromosome 21 was performed in 188 AD and 375 controls, using 417 SNPs at an average interval of <100 kb, including at least one SNP in each coding region. Selected SNP markers were distributed between base positions 14 440 543 and 46 915 057 based on NCBI Build 35, whereas no SNP closer to the centromere was included because of the duplicated region in the chromosome 21 sequence (18). Using a threshold of $P < 0.05$ for allele frequency, we detected 14 SNPs, which is less than the predicted 21 markers. Therefore, to reduce type II error, we also tested genotype frequency in both dominant and recessive models (Fig. 1). Finally, the exploratory scan detected 42 SNPs in total (10.0%), among which 14 SNPs were significant in both allele and genotype frequencies, of which one positive region was identified in the Down syndrome critical region (DSCR) (19–21). The confirmatory scan targeting the selected 42 SNPs indicated that 22 SNPs were still significant for either allele or genotype frequency (Table 1). Among those, 17 SNPs were also significant by logistic regression for the risk genotype with age, sex and APOE-ε4 dose. Genes linked to these SNPs were the

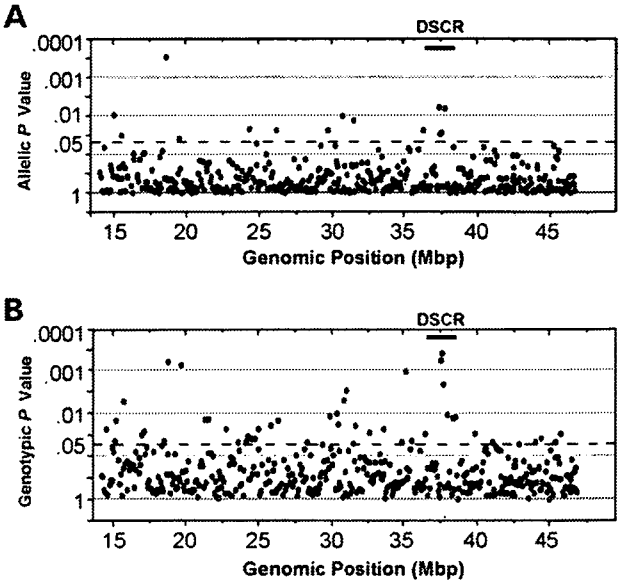

Figure 1. Exploratory scan using 417 markers. (**A**) *P*-values for allele frequency in chi-squared test. (**B**) *P*-values for genotype frequency in better fitting models. Genomic position is based on NCBI Build 35.

SAMSN1, *PRSS7*, *NCAM2*, *RUNX1*, *DYRK1A* and *KCNJ6* genes and those linked to unknown open reading frames were C21ORF 63, 55 and 5. In logistic regression, the *DYRK1A* gene, located in the middle of the DSCR, showed the highest significance [OR = 2.99 (95% CI: 1.72–5.19), $P = 0.001$], whereas the *RUNX1* gene showed a very high odds ratio [OR = 23.3 (95% CI: 2.76–196.5), $P = 0.038$].

Haplotype analysis of *DYRK1A*

SNPs located in the *DYRK1A* gene region were genotyped to determine the haplotype associated with AD. Linkage disequilibrium was identified in the control group from 30 kb upstream of exon 1 to intron 9, but not in exon 13 genotyped by rs1803439 which was not in Hardy–Weinberg equilibrium, and the AD group showed similar results (Fig. 2). Haplotype analysis indicated that three haplotypes had significantly different frequencies between AD and controls, whereas the permutation test supported significant differences in two haplotypes. Considering the haplotype frequencies, rs8126696 alleles could represent the risk haplotype (Table 2). We also sequenced all coding regions of the *DYRK1A* gene in six patients and three controls homozygous for the risk allele, but no sequence alteration was found.

DYRK1A mRNA in hippocampus of AD

DYRK1A mRNA in the hippocampus was measured by quantitative polymerase chain reaction (PCR) to examine the relation with the occurrence of AD and with the genotype of rs8126696. *DYRK1A* mRNA level in the patients was significantly different ($P < 0.01$), being ~7-fold greater than that in pathological controls (Fig. 3A). In contrast, patients homozygous for the risk rs8126696-c allele showed a tendency for a decrease in *DYRK1A* mRNA level compared with the others,

Table 1. Genes linked to markers associated with AD on chromosome 21

Marker	Association[a] (*P*)		Logistic regression[b]		Gene
	Allele	Genotype[c]	Odds (95% CI)	*P*-value	
rs723856	0.019	0.012 (aa)	1.53 (1.08–2.18)	0.0181	*SAMSN1*
rs2268437	0.008	0.008 (aa)	2.09 (1.24–3.55)	0.0059	*PRSS7*
rs2212624[d]	0.058	0.003 (gg)	1.66 (1.17–2.35)	0.0046	*NCAM2*
rs2833844	0.033	0.030 (cc)	1.74 (1.11–2.73)	0.0166	C21 orf 63
rs28360609[d]	0.128	0.017 (aa)	3.43 (1.31–8.95)	0.0119	C21 orf 55
rs4816501	0.224	0.004 (tt)	23.3 (2.76–196.5)	0.0038	*RUNX1*
rs1023367	0.054	0.036 (cc, ct)	1.40 (0.96–2.05)	0.0839	C21 orf 5
rs2835740	0.035	0.001 (cc)	2.99 (1.72–5.19)	0.0001	*DYRK1A*
rs2835908	0.024	0.056 (cc)	1.55 (0.99–2.43)	0.0546	*KCNJ6*

[a]One-sided *P*-value in chi-squared test.
[b]Logistic regression of risk genotype with age, sex and APOE-ε4 dose under no interaction.
[c]Risk genotypes in a better fitting model are shown in parentheses.
[d]AD group showed deviation from the Hardy–Weinberg equilibrium.

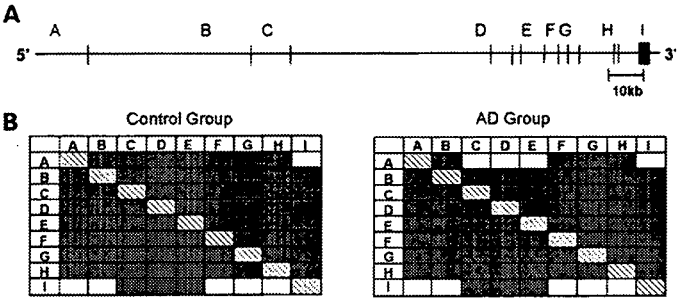

Figure 2. Linkage disequilibrium in *DYRK1A* gene region. (**A**) Genomic structure of the *DYRK1A* gene is shown. Horizontal bar indicates exons, and letters indicate SNPs, such as rs28360609 (A), rs2251085 (B), rs2835740 (C), rs10470178 (D), rs11701810 (E), rs1024294 (F), rs2835773 (G), rs2835774 (H) and rs1803439 (I). (**B**) r^2 (upper right) and $|D'|$ values (lower left) were judged significant at less than 0.5 and 0.9, respectively, and significant values are shown by dark boxes.

Table 2. Haplotype case–control study for *DYRK1A* gene

Haplotype[a]	Frequency			*P*-value	
	Overall	AD	Control	Chi-squared	Permutation
2-1-2-1-1-1-2-1	0.500	0.467	0.532	0.0147	0.013
1-2-1-2-2-2-1-2	0.312	0.337	0.287	0.0395	0.051
1-2-2-1-1-2-1-2	0.065	0.064	0.067	0.8369	0.844
1-1-2-1-1-1-2-1	0.065	0.080	0.050	0.0216	0.017
2-1-2-1-1-1-2-1	0.031	0.025	0.038	0.1582	0.171
1-2-1-2-2-2-1-2	0.016	0.018	0.015	0.6984	0.745
1-2-2-2-2-2-1-2	0.011	0.010	0.013	0.6268	0.632

[a]Haplotypes were constructed with markers composed of rs8126696 (allele 1 = c, allele 2 = t)–rs2251085 (c/g)–rs2835740 (c/t)–rs10470178 (a/g)–rs11701810 (a/c)–rs1024294 (c/t)–rs2835773 (a/g)–rs2835774 (a/t). Chi-squared for the overall haplotypes (df = 6) was significant by the EM algorithm ($P = 0.040$) as well as by the permutation method ($P = 0.038$).

but this was not significant (Fig. 3B). Thus, the increased expression of *DYRK1A* mRNA is possibly a consequence of AD.

DYRK1A mRNA and Aβ in transgenic mouse brain

We examined whether Aβ loading is related to *DYRK1A* mRNA level in the brain in PS1^{I213T}KI and Tg-PS1/APP mice. Aβ1–40 level in PS1^{I213T}KI mice was low, but Aβ1–40 was almost undetectable, whereas both Aβ1–40 and Aβ1–42 were elevated in Tg-PS1/APP mice (Fig. 4A and B), suggesting that Tg-PS1/APP mice have an Aβ burden in their brain. Quantitative PCR showed that the *DYRK1A* mRNA level was significantly increased in Tg-PS1/APP mice when compared with that in PS1^{I213T}KI mice ($P < 0.05$) by 1.2-fold (Fig. 4C). Thus, the expression of *DYRK1A* mRNA increased along with Aβ loading in the mouse brain.

DYRK1A mRNA, Aβ and tau phosphorylation in cell models

We examined whether Aβ, a major component of senile plaques in the AD brain, induces expression of *DYRK1A* mRNA in cultured neuroblastoma cells. SH-SY5Y cells were incubated with Aβ, and then total RNA was extracted and quantified (Fig. 5). *DYRK1A* mRNA level was significantly increased by 1.6-fold ($P < 0.05$) with 0.5 μM Aβ1–42 and by 1.3-fold ($P < 0.01$) with 25 μM Aβ25–35, compared with the level in non-treated cells, but was not changed with control 25 μM Aβ35-25. Thus, Aβ loading resulted in an increase in the *DYRK1A* transcription. In an *in vitro* experiment, DYRK1A protein not only phosphorylates itself, but also has a large repertoire of phosphorylation (22). Therefore, we examined whether *DYRK1A* overexpression induces phosphorylation of tau at the cellular level. An immunoblot of HEK293T cells transiently transfected with the *MAPT* expression vector showed a detectable amount of tau along with those phosphorylated at Thr^{212} (Fig. 6A). Tau phosphorylated at Thr^{212} was increased by co-transfection of the *DYRK1A* expression vector, compared with that of mock vector, whereas tau level was similar (Fig. 6A). Densitometric quantification supported the induction of phosphorylation by 1.5-fold ($P < 0.01$) (Fig. 6B). Thus, the increase in the *DYRK1A* transcription under overexpression of tau induced tau phosphorylation at Thr^{212}.

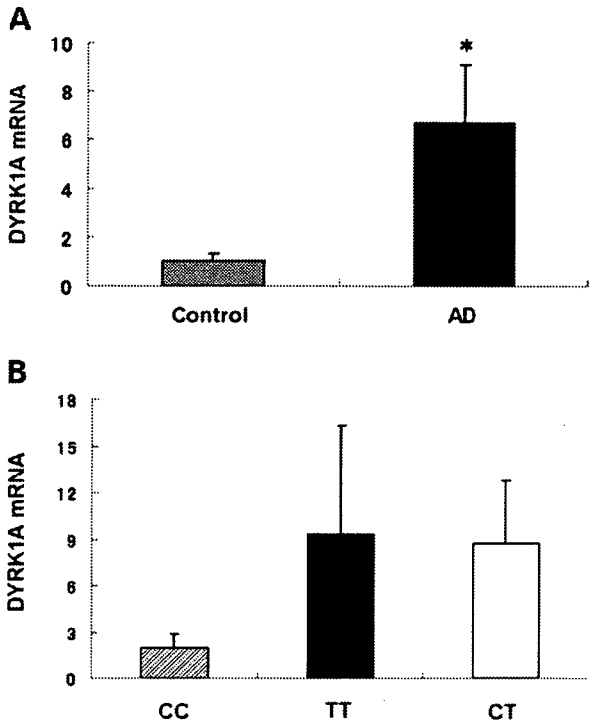

Figure 3. Expression of *DYRK1A* mRNA in human hippocampus. (**A**) Quantitative real-time PCR of *DYRK1A* mRNA in AD ($n = 22$) and controls ($n = 12$). (**B**) *DYRK1A* mRNA level in AD brain divided by rs28360609 genotypes, where CC is the risk genotype. *DYRK1A* mRNA level was expressed as the ratio of that of *GAPDH*. Data are shown as mean ± SEM. $^{*}P < 0.01$ by Mann–Whitney's *U*-test.

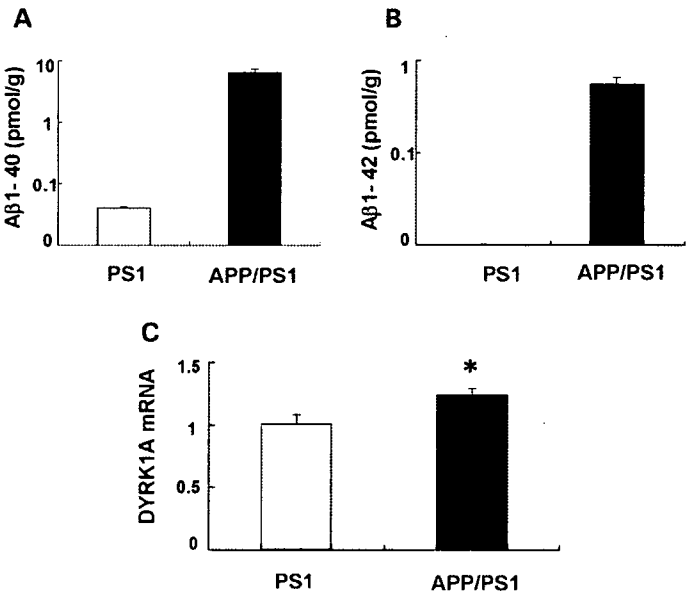

Figure 4. Aβ-level and expression of *DYRK1A* mRNA in transgenic mouse brain. Heterozygous PS1^{I213T}KI (PS1, $n = 6$) and Tg-APP/PS1 (APP/PS1, $n = 6$) mice were sacrificed at 9 months of age. Aβ-level was measured by ELISA. *DYRK1A* mRNA level was measured by quantitative real-time PCR. (**A**) Aβ1–40 level, (**B**) Aβ1–42 level and (**C**) amount of *DYRK1A* mRNA. *DYRK1A* mRNA level was expressed as the ratio of that of *GAPDH*. Data are shown as mean ± SEM. $^{*}P < 0.01$ by Student's *t*-test.

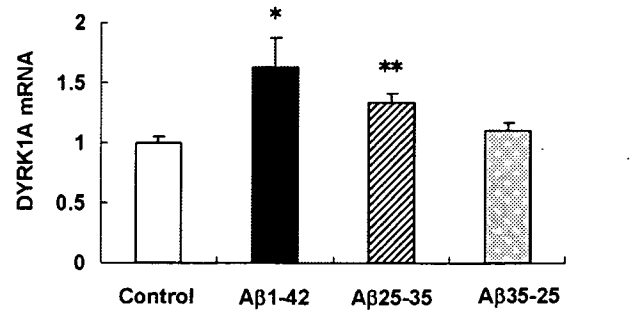

Figure 5. Aβ-induced expression of *DYRK1A* mRNA in SH-SY5Y cells. SH-SY5Y cells were incubated with Aβ1–42, Aβ25–35 and Aβ35–25. *DYRK1A* mRNA level was measured by quantitative real-time PCR. Values were normalized to those in untreated cells. *DYRK1A* mRNA level was expressed as the ratio of that of *GAPDH*. Data are shown as mean ± SEM of four independent measurements. $^{**}P < 0.01$ and $^{*}P < 0.05$ by Student's *t*-test compared with control.

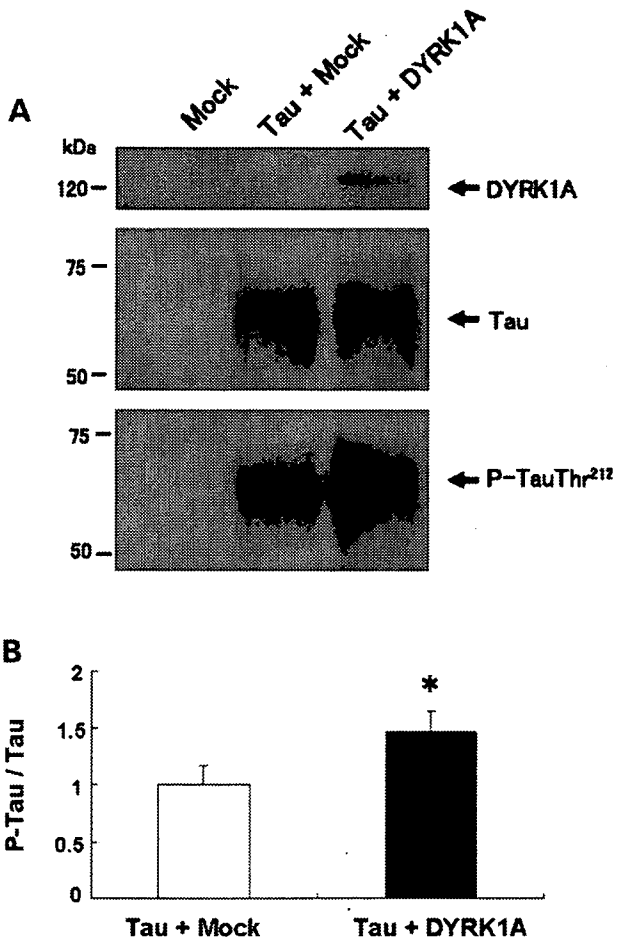

Figure 6. Tau hyperphosphorylation in DYRK1A-overexpressing cells. (**A**) HEK293T cells were transfected with either the *MAPT* expression vector (Tau) or both the *MAPT* and *DYRK1A* expression vectors (Tau + DYRK1A). After 24 h incubation, lysates were immunoprecipitated with anti-FLAG M2 agarose and then subjected to immunoblotting with anti-DYRK1A (DYRK1A), anti-tau (Tau) or anti-phosphotau (P-TauThr^{212}). (**B**) P-TauThr^{212}/Tau ratio was measured as integrated optical density values. Data are shown as mean ± SEM of four independent measures. $^{*}P < 0.01$ by Student's *t*-test.

Discussion

Genome scanning using case–control studies, based on linkage disequilibrium, is a strategy to identify genetic factors of polygenetic diseases. In general, many susceptibility genes have been reported, but it remains difficult to replicate the results in different studies. This could possibly be caused by selection bias in patients as well as in controls, because hospital-based control subjects often suffer from another disease, leading to an additional background of that disease. Therefore, we used population-based controls to match the phenotypic background. From the exploratory and confirmatory scans, we identified 22 candidate SNPs associated with late-onset AD on chromosome 21. Although we showed their risk effects in logistic regression with age, sex and *APOE*-ε4 dose, a known major risk for AD (3), these candidates need to be confirmed, because *P*-values were inconclusive when considering the comparison of multiple loci.

We found associations of AD with markers linked to six known genes, but not with reported candidates, the *APP* and *BACE2* genes. The *SAMSN1* gene encodes a member of putative adaptors and scaffold proteins containing SH3 and sterile alpha motif domains, expressed mainly in immune tissues and hematopoietic cells and also at lower levels in the heart, brain, placenta and lung (23). The *DYRK1A* gene, located in the DSCR, is a candidate gene responsible for learning and memory impairment in patients with DS (24,25). The *PRSS7* gene encodes enteropeptidase (EC 3.4.21.9), an intestinal enzyme initiating activation of pancreatic proteolytic proenzymes such as trypsin, chymotrypsin and carboxypeptidase A, which are highly expressed in the intestines and at a low level in the brain of rat (26), but is downregulated in amniotic fluid cells in patients with DS (27). The neural cell adhesion molecule 2 (*NCAM2*) gene is expressed in fetal and adult brains (28), sharing many features with immunoglobulins and mediating adhesion among neurons and between neurons and muscle (29) and having a potential regulatory role in the formation of selective axonal projections of olfactory sensory neurons in mice (30). The *RUNX1* gene, also called *AML1*, encodes runt-related transcription factor 1, which is required for active repression in CD4-negative/CD8-negative thymocytes, and a defective *RUNX1* gene causes a familial platelet disorder with predisposition to acute myelogenous leukemia (31). The mouse *RUNX1* homolog is expressed in selected populations of post-mitotic neurons of the embryonic central and peripheral nervous systems (32). The *KCNJ6* gene, located in the DSCR, encodes a G protein-coupled inwardly rectifying potassium channel and is expressed in the brain and pancreatic beta cells (33,34). A *kcnj6* mutation was found in the weaver mouse characterized by ataxia with reduced size of the cerebellum because of depletion of granule cell neurons (35).

DYRK1A is a mammalian ortholog of the *Drosophila minibrain* gene, which is essential for normal post-embryonic neurogenesis (36). In rodents, *DYRK1A* mRNA is expressed ubiquitously in various tissues during development and is also strongly expressed in the adult brain and heart (20, 37–39). In humans, *DYRK1A* mRNA is expressed especially in the brain, and immunoreactive DYRK1A is found in the cerebral cortex, hippocampus and cerebellum and is overexpressed in the DS brain in a dose-dependent manner (40,41). Transgenic mice overexpressing full-length *DYRK1A* mRNA exhibit neurodevelopmental delay, motor abnormalities and cognitive deficit, suggesting a causative role of the *DYRK1A* gene in mental retardation and motor anomalies of DS (24,25). It was noted that all adults with DS over the age of 40 years develop sufficient neuropathology for a diagnosis of AD (42). The identification of the *DYRK1A* gene as a genetic factor strongly supports that the *DYRK1A* gene is involved in the development of AD.

We demonstrated an increase in the *DYRK1A* mRNA level in post-mortem brains, coinciding with the recent report of DYRK1A immunoreactivity in the neocortex and hippocampus in AD (41). The risk genotype of the *DYRK1A* gene showed a tendency for a decrease in the *DYRK1A* mRNA level, but our observation needs to be carefully considered because the result might be caused by the reduction of neuronal cells in the AD brain. However, no studies have yet examined the relationship between the *DYRK1A* gene and Aβ. Genetic and pathological evidence strongly supports the amyloid cascade hypothesis that Aβ42, a proteolytic derivative of the APP protein, has an early and pivotal role in all cases of AD. It is thought that Aβ42 forms aggregates that initiate the pathogenic cascade, leading ultimately to neural loss and dementia (43). We demonstrated that Aβ, especially Aβ42, results in an increase of *DYRK1A* transcription in human neuroblastoma cells and is also observed in transgenic mouse models. Therefore, the increase in *DYRK1A* transcription is a common feature of AD and DS and could relate to the cognitive impairment in patients with AD.

The DYRK1A enzyme has dual substrate specificity: autophosphorylation for self-activation takes place on the Tyr^{321} residue in the active loop of the catalytic domain (44) and target protein phosphorylation occurs on serine/threonine residues in several proteins, including STAT3, FHKR, Gli-1, eIF2Bε, tau, dynamin, glycogen synthase, 14-3-3, CREB, cyclin L2, Arip4, Hip-1 and PAHX-AP1, indicating that DYRK1A may participate in many biological pathways (22). We showed that overexpression of the *DYRK1A* gene phosphorylates tau at Thr^{212} in HEK293T cells overproducing tau, suggesting that tau phosphorylation at Thr^{212} by DYRK1A could be a downstream consequence of Aβ overproduction. It was shown in an *in vitro* experiment that DYRK1A phosphorylates tau at Thr^{212}, which primes tau for phosphorylation by GSK3-β at Ser^{208}, leading to the formation of paired helical filaments composed of highly phosphorylated tau, a component of neurofibrillary tangles (41). However, transgenic mice overexpressing DYRK1A did not show this phosphorylation, and this phosphorylation is highly susceptible to dephosphorylation by protein phosphatase-1, which is expressed in the frontal lobes of the brain, indicating that tau phosphorylation at Thr^{212} could be prohibited *in vivo* (45,46). On the contrary, it was noted that peptides of tau phosphorylated at Thr^{212} completely block Aβ binding, and DYRK1A mediated phosphorylation of Huntingtin-interacting protein 1 (Hip-1) in response to βFGF, resulting in the blockade of Hip-1-mediated neuronal cell death as well as the enhancement of neurite outgrowth (47,48). Therefore, tau phosphorylation at Thr^{212} could be a protective response against neuronal cell death. Although overexpression of DYRK1A could be a common phenomenon

between AD and DS, neuropathological studies might elucidate how the pathway from overexpression of DYRK1A to phosphorylation of tau is related to the severity of Alzheimer pathology.

Our study provides evidence that the *DYRK1A* gene is a genetic factor for AD, whose expression is increased by Aβ loading in neuroblastoma cells and transgenic mice, resulting in hyperphosphorylation of tau at Thr^{212} under overexpression of tau. The *DYRK1A* gene could be responsible for learning and memory deterioration in DS (24,25), and a DYRK1A inhibitor has been proposed as a novel drug to address learning and memory deficit in DS (49). Our findings suggest that *DYRK1A* upregulation is a key phenomenon as a consequence of Aβ loading in AD, connecting the condition to DS, and we propose a possible relation between the *DYRK1A* gene and memory impairment in AD.

MATERIALS AND METHODS

Sample-set characteristics

Patients with late-onset AD were diagnosed as having definite or probable AD according to the criteria of the National Institute of Neurological and Communicative Disorders and Stroke–Alzheimer's Disease and Related Disorders Association (50). Non-demented control subjects, tested by a questionnaire including the date, orientation and past history, were obtained from population-based elderly subjects. Written informed consent to participate in this study was obtained, and then peripheral blood was drawn and subjected to DNA extraction. The number of patients for the scan was 374 (70.6% female), composed of 73 with definite and 301 with probable AD; mean ± SD age at onset was 73.0 ± 8.0, range 60–94 years and age at blood drawing was 78.2 ± 8.3, range 60–98 years. Controls were composed of 375 individuals (54.7% female); age at assessment was 75.5 + 4.85, range 66–92 years. Brain hippocampal tissue was also obtained from the post-mortem brains of 22 patients with AD (age: 82.8 ± 8.5 years, 63.6% female) and 12 pathological controls (age: 89.0 ± 7.0 years, age at onset: 72.9 ± 7.2 years and 58.0% female). DNA was extracted from peripheral blood nuclear cells by phenol–chloroform method or using a QIAamp DNA Blood Kit (Qiagen, Tokyo, Japan). The procedure to obtain the specimens was approved by the Genome Ethical Committee of Osaka University Graduate School of Medicine, Ehime University and the Ethical Committee of Fukushimura Hospital.

Genotyping and sequencing

An exploratory scan was performed in 188 patients (67.0% female) (age at onset: 75.0 ± 7.2 and range 60–92 years) and 375 controls matched for age. A confirmatory scan was performed in 374 patients including 175 who underwent exploratory scan, and the data were compared with the genotype data of controls in the exploratory scan. The whole genomic DNA was amplified by degenerate oligonucleotide-primed-PCR and used in the confirmatory scan, because of the small amount of DNA (51). The accuracy of genotyping in the confirmatory scan was monitored by comparison with data obtained in the exploratory scan. The selected markers were 417 SNPs distributed in chromosome 21, spanning a region of 33 Mb, which was sequenced and reported by the Chromosome 21 Mapping and Sequencing Consortium (18). Mean interval of the markers in NCBI Build 35 was 78.1 kb, and their range was 7.7–240.0 kb, and 15 intervals were over 100 kb where no coding region was predicted on the basis of the SNP information in using SNPbrowser Software Version 3.5 on NCBI Build 35, available from http://www.appliedbiosystems.com/. Genotyping was performed by a quantitative genotyping method using the TaqMan SNP Genotyping System (Applied Biosystems, Foster City, CA, USA). DNA obtained from six patients and three controls homozygous for the risk genotype of the *DYRK1A* gene was subjected to direct sequencing of its exons, using the primers listed in Table 3.

Table 3. Primer sequences for *DYRK1A* gene

Exon	Primer sequences (5′–3′) Forward	Reverse	Product size (bp)
1	gtttttcttcacacagtg	cccccactaactgct	207
1	gtttttcttcacacagtg	cccccactaactgct	207
2	atgtcaaatgatacaaaca	ttttcccaatccataatc	394
3	gcaggttacagaagaggga	agggtaaataggtcacact	258
4	ctcaaatgtcaactgtag	aacaacaagattcactaag	359
5	ttgaatagaaatagatggc	tgtccaacagaaataaaca	445
6	taactgaactctgcgtttg	atacctacactgtcctacc	471
7	gaagttaatcaatggaac	tattcaaactgacctcac	413
8	ctgtatgctggatgtct	aacacactgatttcaagt	372
9	attatgtgagtgtttacg	gtaactgctccccac	481
10	ttaaccagacttcattgt	gtcattctaaaggcacct	433
11	tgaatgtatttgggattttgtgt	actgtgactgggatgtgg	1063
11	tatttgggattttgtg		(For sequencing)
11	ctgctcctcttgg		(For sequencing)
11	caagattctatggagg		(For sequencing)
11	cgtctactccaatcc		(For sequencing)

Quantitative real-time PCR

Total RNA was isolated from frozen brains using the acid guanidine–phenol–chloroform RNA extraction method provided as ISOGEN (Nippon Gene, Toyama, Japan), and purified using an RNAeasy Mini kit (Qiagen). RNA samples with an A_{260}/A_{280} absorption ratio over 1.9 were subjected to cDNA synthesis using a High-Capacity cDNA Archive Kit (Applied Biosystems). Quantitative real-time PCR was carried out in an ABI PRISM 7900HT (Applied Biosystems), and primers/probe sets for the *DYRK1A* and *GAPDH* genes of human and mouse were purchased from TaqMan Gene Expression Assay Products (Applied Biosystems). All quantitative PCR reactions were duplicated, and the ratio of the amount of *DYRK1A* cDNA to that of *GAPDH* internal control cDNA at a threshold in the mid-log phase of amplification was used to compare the amount of *DYRK1A* mRNA.

Transgenic mice

The $PS1^{I213T}KI$ mouse, with a 'knocked-in' human *PS1* I213T mutation in the mouse presenilin 1 gene (52,53), was bred with Tg2576 mice expressing the human *APP* gene harboring

the K670N/M671L Swedish mutation (Taconic) (54). PS1^{I213T}KI and double transgenic (Tg-APP/PS1) mice were maintained on the B6 background. Six heterozygous Tg-APP/PS1 and six PS1^{I213T}KI mice were sacrificed at age 9 months under anesthesia, and their brains were dissected and stored at −80°C until use. All animal procedures were reviewed by the Institutional Animal Care and Use Committee of Shionogi & Co., Ltd. Every effort was made to minimize the number of animals used and their suffering.

Cell culture

Human neuroblastoma (SH-SY5Y) cells were grown in F12 medium (Invitrogen, Carlsbad, CA, USA) with 10% fetal bovine serum (FBS) (JRH Bioscience, Lenexa, KS, USA), and human embryonic kidney (HEK293T) cells were grown in Dulbecco's modified Eagle's medium (Invitrogen) with 10% FBS. Amyloid peptides (Sigma-Aldrich, St Louis, MO, USA) were dissolved in phosphate-buffered saline, followed by incubation at 37°C for 72 h. SH-SY5Y cells were incubated for 20 h with Aβ at 0.5 μM for Aβ1–42 and at 25 μM for Aβ25–35 and Aβ35–25. Total RNA was isolated from harvested cells using an RNAeasy Mini kit, and then synthesized cDNA was subjected to quantitative PCR. The human long isoform of *MAPT* cDNA, obtained from Dr Goedert (Medical Research Council Laboratory of Molecular Biology, Cambridge, UK), was cloned in pcDNA3.1 (Invitrogen), and the FLAG epitope-tagged *DYRK1A* expression vector was cloned in pEGFPC2 (55,56). These vectors were transfected into HEK293T cells using Lipofectamine 2000 (Invitrogen) in Opti-MEM (Invitrogen), followed by their expression for 24 h, and the cells were harvested and subjected to biochemical experiments.

Biochemical experiments

In transgenic mice, the hemisphere of each brain was homogenized in Tris-buffered saline (TBS) composed of 137 mM NaCl and 20 mM Tris, pH 7.6, containing 1% Triton X-100 with Complete™ protease inhibitor (Roche Diagnostics, Indianapolis, IN, USA), followed by ultracentrifugation, and the supernatant was subjected to measurement of Aβ1–40 and Aβ1–42 levels using a sandwich ELISA kit (Biosource International, Camarillo, CA, USA). In cell experiments, cells were lysed in lysis buffer composed of 150 mM NaCl, 50 mM Tris, pH 8.0, 1% NP-40, 0.1% sodium dodecyl sulfate (SDS), 0.5% sodium deoxycholate, protease inhibitor mixture (Sigma-Aldrich) and phosphatase inhibitor cocktail (Pierce, Rockford, IL, USA). After centrifugation at 10 000*g* for 15 min at 4°C, protein extracts were obtained as the supernatant and quantified using BCA Protein Assay (Pierce). For immunoprecipitation, 300 μg of protein lysate was incubated with 20 μl anti-FLAG M2 agarose (Sigma-Aldrich) with gentle rotation at 4°C overnight, and after centrifugation, the precipitate was dissolved in SDS sample buffer, electrophoresed in 8% SDS–PAGE and blotted onto nitrocellulose membranes (GE Healthcare Bio-Sciences, Piscataway, NJ, USA). After blocking with 5% milk in TBS buffer composed of 0.1% Tween-20, 140 mM NaCl and 10 mM Tris–HCl, pH 7.6, the membranes were incubated overnight at 4°C with primary antibodies, such as polyclonal antibody to phosphotau (P-TauThr^{212}) (Biosource International) diluted to 1:500 or polyclonal antibodies to DYRK1A (Abcam, Cambridge, MA, USA) at 1:200 or to tau (Santa Cruz Biotechnology, Santa Cruz, CA, USA) at 1:500. The membranes were washed and then incubated with peroxidase-conjugated secondary antibodies against mouse, rabbit or sheep immunoglobulin (Promega, Madison, WI, USA), followed by washing and developing with an ECL Plus Western Blotting Detection System (GE Healthcare Bio-Sciences). The immunoreactive bands on films were digitized with an HP 2355 and subjected to densitometric quantification using Image J version 1.36 (National Institute of Health).

Statistical analysis

To reduce type II errors, the exploratory and confirmatory scans were assessed for associations by one-sided chi-squared test for both allele and genotype frequencies in dominant and recessive models, where each α-level was 0.05. For markers showing significant associations in the confirmatory scan, the Hardy–Weinberg equilibrium was tested. The risk genotypes in the better fitting model were given a value of 1 and the other genotypes 0, and then logistic regression was performed along with age, sex and the *APOE*-ε4 dose under no interaction, using StatView software (SAS Institute, Cary, NC, USA). Linkage disequilibrium in the *DYRK1A* gene was also assessed by $|D'|$ and r^2 values; those less than 0.9 and 0.5, respectively, were judged significant (57). Case–control haplotype analysis was performed with the EM algorithm (58) and with the permutation test at 1000 iterations (59), using SNPAlyze software (DYNACOM, Japan). Normally distributed variables were compared by Student's *t*-test; otherwise non-parametric Mann–Whitney's *U*-test was applied. A *P*-value less than 0.05 was considered significant.

ACKNOWLEDGEMENTS

We thank Drs Y. Ikejiri, T. Nishikawa, H. Yoneda, Y. Moto, A. Sawa, S. Fujinaga, T. Matsubayashi, K. Taniguchi, Y. Ikemura, T. Mori and J. Okuda for clinical evaluation and E. Miyamura for assistance. This work was funded by the Future Program and the Japan Society for the Promotion of Science (JSPS) and by a Grant-in-Aid for Scientific Research on Priority Areas 'Applied Genomics' from the Ministry of Education, Culture, Sports, Science and Technology of Japan.

Conflict of Interest statement. None of the authors has any conflict of interest.

REFERENCES

1. Sorbi, S., Forleo, P., Tedde, A., Cellini, E., Ciantelli, M., Bagnoli, S. and Nacmias, B. (2001) Genetic risk factors in familial Alzheimer's disease. *Mech. Ageing Dev.*, **122**, 1951–1960.
2. Wisniewski, K.E., Wisniewski, H.M. and Wen, G.Y. (1985) Occurrence of neuropathological changes and dementia of Alzheimer's disease in Down's syndrome. *Ann. Neurol.*, **17**, 278–282.
3. Corder, E.H., Saunders, A.M., Strittmatter, W.J., Schmechel, D.E., Gaskell, P.C., Small, G.W., Roses, A.D., Haines, J.L. and

Pericak-Vance, M.A. (1993) Gene dose of apolipoprotein E type 4 allele and the risk of Alzheimer's disease in late onset families. *Science*, **261**, 921–923.
4. Farrer, L.A., Cupples, L.A., Haines, J.L., Hyman, B., Kukull, W.A., Mayeux, R., Myers, R.H., Pericak-Vance, M.A., Risch, N. and van Duijn, C.M. (1997) Effects of age, sex, and ethnicity on the association between apolipoprotein E genotype and Alzheimer disease. A meta-analysis. APOE and Alzheimer Disease Meta Analysis Consortium. *JAMA*, **278**, 1349–1356.
5. Rovelet-Lecrux, A., Hannequin, D., Raux, G., Le Meur, N., Laquerriere, A., Vital, A., Dumanchin, C., Feuillette, S., Brice, A., Vercelletto, M. *et al.* (2006) APP locus duplication causes autosomal dominant early-onset Alzheimer disease with cerebral amyloid angiopathy. *Nat. Genet.*, **38**, 24–26.
6. Li, L., Perry, R., Wu, J., Pham, D., Ohman, T., Harrell, L.E., Go, R.C. and Fukuchi, K. (1998) Polymorphic tetranucleotide repeat site within intron 7 of the β-amyloid precursor protein gene and its lack of association with Alzheimer's disease. *Hum. Genet.*, **103**, 86–89.
7. Athan, E.S., Lee, J.H., Arriaga, A., Mayeux, R.P. and Tycko, B. (2002) Polymorphisms in the promoter of the human APP gene: functional evaluation and allele frequencies in Alzheimer disease. *Arch. Neurol.*, **59**, 1793–1799.
8. Clarimon, J., Bertranpetit, J., Calafell, F., Boada, M., Tarraga, L. and Comas, D. (2003) Joint analysis of candidate genes related to Alzheimer's disease in a Spanish population. *Psychiatr. Genet.*, **13**, 85–90.
9. Nowotny, P., Kwon, J.M., Chakraverty, S., Nowotny, V., Morris, J.C. and Goate, A.M. (2001) Association studies using novel polymorphisms in BACE1 and BACE2. *Neuroreport*, **12**, 1799–1802.
10. Myllykangas, L., Wavrant-De Vrieze, F., Polvikoski, T., Notkola, I.L., Sulkava, R., Niinisto, L., Edland, S.D., Arepalli, S., Adighibe, O., Compton, D. *et al.* (2005) Chromosome 21 BACE2 haplotype associates with Alzheimer's disease: a two-stage study. *J. Neurol. Sci.*, **236**, 17–24.
11. Li, Y., Hollingworth, P., Moore, P., Foy, C., Archer, N., Powell, J., Nowotny, P., Holmans, P., O'Donovan, M., Tacey, K. *et al.* (2005) Genetic association of the APP binding protein 2 gene (APBB2) with late onset Alzheimer disease. *Hum. Mutat.*, **25**, 270–277.
12. Kehoe, P., Wavrant-De Vrieze, F., Crook, R., Wu, W.S., Holmans, P., Fenton, I., Spurlock, G., Norton, N., Williams, H., Williams, N. *et al.* (1999) A full genome scan for late onset Alzheimer's disease. *Hum. Mol. Genet.*, **8**, 237–245.
13. Myers, A., Wavrant-De Vrieze, F., Holmans, P., Hamshere, M., Crook, R., Compton, D., Marshall, H., Meyer, D., Shears, S., Booth, J. *et al.* (2002) Full genome screen for Alzheimer disease: stage II analysis. *Am. J. Med. Genet.*, **114**, 235–244.
14. Wu, W.S., Holmans, P., Wavrant-DeVrieze, F., Shears, S., Kehoe, P., Crook, R., Booth, J., Williams, N., Perez-Tur, J., Roehl, K. *et al.* (1998) Genetic studies on chromosome 12 in late-onset Alzheimer disease. *JAMA*, **280**, 619–622.
15. Pericak-Vance, M.A., Grubber, J., Bailey, L.R., Hedges, D., West, S., Santoro, L., Kemmerer, B., Hall, J.L., Saunders, A.M., Roses, A.D. *et al.* (2000) Identification of novel genes in late-onset Alzheimer's disease. *Exp. Gerontol.*, **35**, 1343–1352.
16. Farrer, L.A., Bowirrat, A., Friedland, R.P., Waraska, K., Korczyn, A.D. and Baldwin, C.T. (2003) Identification of multiple loci for Alzheimer disease in a consanguineous Israeli-Arab community. *Hum. Mol. Genet.*, **12**, 415–422.
17. Holmans, P., Hamshere, M., Hollingworth, P., Rice, F., Tunstall, N., Jones, S., Moore, P., Wavrant-DeVrieze, F., Myers, A., Crook, R. *et al.* (2005) Genome screen for loci influencing age at onset and rate of decline in late onset Alzheimer's disease. *Am. J. Med. Genet. B. Neuropsychiatr. Genet.*, **135**, 24–32.
18. The Chromosome 21 Mapping Sequencing Consortium (2000) The DNA sequence of human chromosome 21. *Nature*, **405**, 311–319.
19. Ohira, M., Ichikawa, H., Suzuki, E., Iwaki, M., Suzuki, K., Saito-Ohara, F., Ikeuchi, T., Chumakov, I., Tanahashi, H., Tashiro, K. *et al.* (1996) A 1.6-Mb P1-based physical map of the Down syndrome region on chromosome 21. *Genomics*, **33**, 65–74.
20. Guimera, J., Casas, C., Pucharcos, C., Solans, A., Domenech, A., Planas, A.M., Ashley, J., Lovett, M., Estivill, X. and Pritchard, M.A. (1996) A human homologue of *Drosophila minibrain* (MNB) is expressed in the neuronal regions affected in Down syndrome and maps to the critical region. *Hum. Mol. Genet.*, **5**, 1305–1310.
21. Shindoh, N., Kudoh, J., Maeda, H., Yamaki, A., Minoshima, S., Shimizu, Y. and Shimizu, N. (1996) Cloning of a human homolog of the *Drosophila minibrain*/rat Dyrk gene from 'the Down syndrome critical region' of chromosome 21. *Biochem. Biophys. Res. Commun.*, **225**, 92–99.
22. Galceran, J., de Graaf, K., Tejedor, F.J. and Becker, W. (2003) The MNB/DYRK1A protein kinase: genetic and biochemical properties. *J. Neural Transm. Suppl.*, **67**, 139–148.
23. Claudio, J.O., Zhu, Y.X., Benn, S.J., Shukla, A.H., McGlade, C.J., Falcioni, N. and Stewart, A.K. (2001) HACS1 encodes a novel SH3-SAM adaptor protein differentially expressed in normal and malignant hematopoietic cells. *Oncogene*, **20**, 5373–5377.
24. Smith, D.J., Stevens, M.E., Sudanagunta, S.P., Bronson, R.T., Makhinson, M., Watabe, A.M., O'Dell, T.J., Fung, J., Weier, H.U., Cheng, J.F. *et al.* (1997) Functional screening of 2 Mb of human chromosome 21q22.2 in transgenic mice implicates minibrain in learning defects associated with Down syndrome. *Nat. Genet.*, **16**, 28–36.
25. Altafaj, X., Dierssen, M., Baamonde, C., Marti, E., Visa, J., Guimera, J., Oset, M., Gonzalez, J.R., Florez, J., Fillat, C. *et al.* (2001) Neurodevelopmental delay, motor abnormalities and cognitive deficits in transgenic mice overexpressing Dyrk1A (minibrain), a murine model of Down's syndrome. *Hum. Mol. Genet.*, **10**, 1915–1923.
26. Yahagi, N., Ichinose, M., Matsushima, M., Matsubara, Y., Miki, K., Kurokawa, K., Fukamachi, H., Tashiro, K., Shiokawa, K., Kageyama, T. *et al.* (1996) Complementary DNA cloning and sequencing of rat enteropeptidase and tissue distribution of its mRNA. *Biochem. Biophys. Res. Commun.*, **219**, 806–812.
27. Chung, I.H., Lee, S.H., Lee, K.W., Park, S.H., Cha, K.Y., Kim, N.S., Yoo, H.S., Kim, Y.S. and Lee, S. (2005) Gene expression analysis of cultured amniotic fluid cell with Down syndrome by DNA microarray. *J. Korean Med. Sci.*, **20**, 82–87.
28. Paoloni-Giacobino, A., Chen, H. and Antonarakis, S.E. (1997) Cloning of a novel human neural cell adhesion molecule gene (NCAM2) that maps to chromosome region 21q21 and is potentially involved in Down syndrome. *Genomics*, **43**, 43–51.
29. Rutishauser, U., Acheson, A., Hall, A.K., Mann, D.M. and Sunshine, J. (1988) The neural cell adhesion molecule (NCAM) as a regulator of cell–cell interactions. *Science*, **240**, 53–57.
30. Alenius, M. and Bohm, S. (2003) Differential function of RNCAM isoforms in precise target selection of olfactory sensory neurons. *Development*, **130**, 917–927.
31. Song, W.J., Sullivan, M.G., Legare, R.D., Hutchings, S., Tan, X., Kufrin, D., Ratajczak, J., Resende, I.C., Haworth, C., Hock, R. *et al.* (1999) Haploinsufficiency of CBFA2 causes familial thrombocytopenia with propensity to develop acute myelogenous leukaemia. *Nat. Genet.*, **23**, 166–175.
32. Theriault, F.M., Roy, P. and Stifani, S. (2004) AML1/Runx1 is important for the development of hindbrain cholinergic branchiovisceral motor neurons and selected cranial sensory neurons. *Proc. Natl Acad. Sci. USA*, **101**, 10343–10348.
33. Sakura, H., Bond, C., Warren-Perry, M., Horsley, S., Kearney, L., Tucker, S., Adelman, J., Turner, R. and Ashcroft, F.M. (1995) Characterization and variation of a human inwardly-rectifying K-channel gene (KCNJ6): a putative ATP-sensitive K-channel subunit. *FEBS Lett.*, **367**, 193–197.
34. Tsaur, M.L., Menzel, S., Lai, F.P., Espinosa, R., III, Concannon, P., Spielman, R.S., Hanis, C.L., Cox, N.J., Le Beau, M.M., German, M.S. *et al.* (1995) Isolation of a cDNA clone encoding a K(ATP) channel-like protein expressed in insulin-secreting cells, localization of the human gene to chromosome band 21q22.1 and linkage studies with NIDDM. *Diabetes*, **44**, 592–596.
35. Patil, N., Cox, D.R., Bhat, D., Faham, M., Myers, R.M. and Peterson, A.S. (1995) A potassium channel mutation in weaver mice implicates membrane excitability in granule cell differentiation. *Nat. Genet.*, **11**, 126–129.
36. Tejedor, F., Zhu, X.R., Kaltenbach, E., Ackermann, A., Baumann, A., Canal, I., Heisenberg, M., Fischbach, K.F. and Pongs, O. (1995) *minibrain*: a new protein kinase family involved in postembryonic neurogenesis in *Drosophila*. *Neuron*, **14**, 287–301.
37. Song, W.J., Sternberg, L.R., Kasten-Sportes, C., Keuren, M.L., Chung, S.H., Slack, A.C., Miller, D.E., Glover, T.W., Chiang, P.W., Lou, L. *et al.* (1996) Isolation of human and murine homologues of the *Drosophila* minibrain gene: human homologue maps to 21q22.2 in the Down syndrome 'critical region'. *Genomics*, **38**, 331–339.

38. Marti, E., Altafaj, X., Dierssen, M., de la Luna, S., Fotaki, V., Alvarez, M., Perez-Riba, M., Ferrer, I. and Estivill, X. (2003) Dyrk1A expression pattern supports specific roles of this kinase in the adult central nervous system. *Brain Res.*, **964**, 250–263.
39. Okui, M., Ide, T., Morita, K., Funakoshi, E., Ito, F., Ogita, K., Yoneda, Y., Kudoh, J. and Shimizu, N. (1999) High-level expression of the Mnb/Dyrk1A gene in brain and heart during rat early development. *Genomics*, **62**, 165–171.
40. Guimera, J., Casas, C., Estivill, X. and Pritchard, M. (1999) Human minibrain homologue (MNBH/DYRK1): characterization, alternative splicing, differential tissue expression, and overexpression in Down syndrome. *Genomics*, **57**, 407–418.
41. Ferrer, I., Barrachina, M., Puig, B., Martinez de Lagran, M., Marti, E., Avila, J. and Dierssen, M. (2005) Constitutive Dyrk1A is abnormally expressed in Alzheimer disease, Down syndrome, Pick disease, and related transgenic models. *Neurobiol. Dis.*, **20**, 392–400.
42. Mann, D.M. and Esiri, M.M. (1989) The pattern of acquisition of plaques and tangles in the brains of patients under 50 years of age with Down's syndrome. *J. Neurol. Sci.*, **89**, 169–179.
43. Selkoe, D.J. (2002) Alzheimer's disease is a synaptic failure. *Science*, **298**, 789–791.
44. Himpel, S., Panzer, P., Eirmbter, K., Czajkowska, H., Sayed, M., Packman, L.C., Blundell, T., Kentrup, H., Grotzinger, J., Joost, H.G. *et al.* (2001) Identification of the autophosphorylation sites and characterization of their effects in the protein kinase DYRK1A. *Biochem. J.*, **359**, 497–505.
45. Woods, Y.L., Cohen, P., Becker, W., Jakes, R., Goedert, M., Wang, X. and Proud, C.G. (2001) The kinase DYRK phosphorylates protein-synthesis initiation factor eIF2Bε at Ser^{539} and the microtubule-associated protein tau at Thr^{212}: potential role for DYRK as a glycogen synthase kinase 3-priming kinase. *Biochem. J.*, **355**, 609–615.
46. Rahman, A., Grundke-Iqbal, I. and Iqbal, K. (2005) Phosphothreonine-212 of Alzheimer abnormally hyperphosphorylated tau is a preferred substrate of protein phosphatase-1. *Neurochem. Res.*, **30**, 277–287.
47. Guo, J.P., Arai, T., Miklossy, J. and McGeer, P.L. (2006) Aβ and tau form soluble complexes that may promote self aggregation of both into the insoluble forms observed in Alzheimer's disease. *Proc. Natl Acad. Sci. USA*, **103**, 1953–1958.
48. Kang, J.E., Choi, S.A., Park, J.B. and Chung, K.C. (2005) Regulation of the proapoptotic activity of huntingtin interacting protein 1 by Dyrk1 and caspase-3 in hippocampal neuroprogenitor cells. *J. Neurosci. Res.*, **81**, 62–72.
49. Kim, N.D., Yoon, J., Kim, J.H., Lee, J.T., Chon, Y.S., Hwang, M.K., Ha, I. and Song, W.J. (2006) Putative therapeutic agents for the learning and memory deficits of people with Down syndrome. *Bioorg. Med. Chem. Lett.*, **16**, 3772–3776.
50. McKhann, G., Drachman, D., Folstein, M., Katzman, R., Price, D. and Stadlan, E.M. (1984) Clinical diagnosis of Alzheimer's disease; report of the NINCDS-ADRDA Work Group under the auspices of Department of Health and Human Services Task Force on Alzheimer's disease. *Neurology*, **34**, 939–944.
51. Sanchez-Cespedes, M., Cairns, P., Jen, J. and Sidransky, D. (1998) Degenerate oligonucleotide-primed PCR (DOP-PCR): evaluation of its reliability for screening of genetic alterations in neoplasia. *Biotechniques*, **25**, 1036–1038.
52. Kamino, K., Sato, S., Sakaki, Y., Yoshiiwa, A., Nishiwaki, Y., Takeda, M., Tanabe, H., Nishimura, T., Ii, K., St George-Hyslop, P.H. *et al.* (1996) Three different mutations of presenilin 1 gene in early-onset Alzheimer's disease families. *Neurosci. Lett.*, **208**, 195–198.
53. Nakano, Y., Kondoh, G., Kudo, T., Imaizumi, K., Kato, M., Miyazaki, J.I., Tohyama, M., Takeda, J. and Takeda, M. (1999) Accumulation of murine amyloidβ42 in a gene-dosage-dependent manner in PS1 'knock-in' mice. *Eur. J. Neurosci.*, **11**, 2577–2581.
54. Hsiao, K., Chapman, P., Nilsen, S., Eckman, C., Harigaya, Y., Younkin, S., Yang, F. and Cole, G. (1996) Correlative memory deficits, Aβ elevation, and amyloid plaques in transgenic mice. *Science*, **274**, 99–103.
55. Goedert, M., Spillantini, M.G., Potier, M.C., Ulrich, J. and Crowther, R.A. (1989) Cloning and sequencing of the cDNA encoding an isoform of microtubule-associated protein tau containing four tandem repeats: differential expression of tau protein mRNAs in human brain. *EMBO J.*, **8**, 393–399.
56. Funakoshi, E., Hori, T., Haraguchi, T., Hiraoka, Y., Kudoh, J., Shimizu, N. and Ito, F. (2003) Overexpression of the human MNB/DYRK1A gene induces formation of multinucleate cells through overduplication of the centrosome. *BMC Cell Biol.*, **4**, 12.
57. Devlin, B. and Risch, N. (1995) A comparison of linkage disequilibrium measures for fine-scale mapping. *Genomics*, **29**, 311–322.
58. Excoffier, L. and Slatkin, M. (1995) Maximum-likelihood estimation of molecular haplotype frequencies in a diploid population. *Mol. Biol. Evol.*, **12**, 921–927.
59. Fallin, D., Cohen, A., Essioux, L., Chumakov, I., Blumenfeld, M., Cohen, D. and Schork, N.J. (2001) Genetic analysis of case/control data using estimated haplotype frequencies: application to APOE locus variation and Alzheimer's disease. *Genome Res.*, **11**, 143–151.

Available online at www.sciencedirect.com
ScienceDirect
Psychiatry Research: Neuroimaging 154 (2007) 133–145
PSYCHIATRY RESEARCH NEUROIMAGING
www.elsevier.com/locate/psychresns

Progressive changes of white matter integrity in schizophrenia revealed by diffusion tensor imaging

Takeyuki Mori[a,b,c,1,2], Takashi Ohnishi[a,b,*,1], Ryota Hashimoto[b,e,f,1,3], Kiyotaka Nemoto[a,1], Yoshiya Moriguchi[a,1], Hiroko Noguchi[b,1], Tetsuo Nakabayashi[b,d,1], Hiroaki Hori[b,1], Seichi Harada[d,1], Osamu Saitoh[d,1], Hiroshi Matsuda[a,c,1,2], Hiroshi Kunugi[b,1]

[a]*Department of Radiology, National Center Hospital for Mental, Nervous, and Muscular Disorders, National Center of Neurology and Psychiatry, 4-1-1 Ogawa Higashi, Kodaira City, Tokyo, 187-8551, Japan*
[b]*Department of Mental Disorder Research, National Institute of Neuroscience, National Center of Neurology and Psychiatry, 4-1-1 Ogawa Higashi, Kodaira City, Tokyo, 187-8551, Japan*
[c]*Department of Nuclear Medicine, Saitama Medical School Hospital. 38 Morohongo Moroyama-machi, Iruma-gun, Saitama, 350-0495, Japan*
[d]*Department of Psychiatry, National Center Hospital for Mental, Nervous, and Muscular Disorders, National Center of Neurology and Psychiatry, 4-1-1 Ogawa Higashi, Kodaira City, Tokyo, 187-8551, Japan*
[e]*The Osaka-Hamamatsu Joint Research Center For Child Mental Development, Osaka University Graduate School of Medicine*
[f]*Department of Psychiatry, Osaka University Graduate School of Medicine*

Received 16 March 2006; received in revised form 6 July 2006; accepted 11 September 2006

Abstract

Recent magnetic resonance imaging (MRI) studies using diffusion tensor imaging (DTI) have suggested reduced fractional anisotropy (FA) in the white matter (WM) of the brain in patients with schizophrenia. We tried to examine whether such reduction in FA exists and whether such changes in FA progress in an age-dependent manner in a Japanese sample of chronic schizophrenia. FA values were compared between 42 patients with chronic schizophrenia and 42 controls matched for age and gender, by using DTI with voxel-by-voxel and region-of-interest analyses. Correlations of FA values with age and duration of illness were examined. Patients with schizophrenia showed lower FA values, compared to controls, in the widespread WM areas including the uncinate fasciculi and cingulum bundles. A significant group-by-age interaction was found for FA in the WM, i.e., age-related reduction of FA was more pronounced in schizophrenics than in controls. A significant negative correlation between FA and duration of illness was also found in the WM. Our data confirmed decreased FA in schizophrenics, compared to controls in the widespread WM areas. Such decreased FA values in schizophrenia might be attributable, at least in part, to progressive changes after the onset of the illness.

Keywords: Magnetic resonance imaging (MRI); DTI; Fractional anisotropy (FA); Aging

* Corresponding author. Department of Radiology, National Center Hospital for Mental, Nervous, and Muscular Disorders, National Center of Neurology and Psychiatry, 4-1-1 Ogawa Higashi, Kodaira City, Tokyo, 187-8551, Japan. Tel.: +81 42 341 2711; fax: +81 42 346 1790.
E-mail address: tohnishi@hotmail.com (T. Ohnishi).
[1] Tel.: +81 42 341 2711.
[2] Tel: +81 49 276 1111.
[3] D3, 2-2, Yamadaoka, Suita City, Osaka, 565-0871, Japan. Tel.: +81 6 6879 3074.

0925-4927/$ - see front matter © 2006 Elsevier Ireland Ltd. All rights reserved.
doi:10.1016/j.pscychresns.2006.09.004

1. Introduction

Diffusion tensor imaging (DTI) (Basser et al., 1994), a newly developed method to estimate the white matter (WM) integrity, provides information about the diffusion of water in biological tissues. In the WM, water diffusion is highly anisotropic, with greater diffusion in the direction parallel to axonal tracts. Thus, diminished anisotropy of water diffusion has been proposed to reflect compromised WM integrity (Lim et al., 1999). Fractional anisotropy (FA) (Basser, 1995) is a quantitative measure of diffusion anisotropy acquired from DTI.

The normally aging brain exhibits an assortment of micro- and macroscopic changes in the WM as well as the cerebral cortex. Histological studies demonstrate a decrease in myelin density and in the number of myelinated fibers (Meier-Ruge et al., 1992). Postmortem brain (Meier-Ruge et al., 1992) and volumetric neuroimaging studies (Christiansen et al., 1994; Salat et al., 1999) have suggested that WM changes are more prominent than cortical changes with aging, at least during certain segments of the age span and in certain regions of the brain. For example, volume loss in prefrontal WM is disproportionately greater than that in prefrontal cortex with late aging {comparison of elderly adults aged 60–75 with those aged >85 years (Salat et al., 1999)}. Several DTI studies have demonstrated age-related reductions of WM anisotropy in the genu of the corpus callosum (Pfefferbaum et al., 2000b), anterior WM (Pfefferbaum et al., 2000a; O'Sullivan et al., 2001), periventricular WM (Nusbaum et al., 2001), and the prefrontal WM (Nusbaum et al., 2001; Pfefferbaum et al., 2005; Salat et al., 2005).

Regarding schizophrenia, impairments of the neural connectivity between certain cortical areas, such as frontal and temporal areas, have been implicated in the pathophysiology of the disease (Frith and Dolan, 1996; Andreasen et al., 1997; Bullmore et al., 1997). Indeed, volumetric magnetic resonance (MR) studies and pathological studies demonstrated abnormalities of the WM in schizophrenia (Miyakawa et al., 1972; Cannon et al., 1998; Davis et al., 2003; Ho et al., 2003; Uranova et al., 2004). Changes in WM integrity in schizophrenia has relevance to the neural disconnection model of the disorder and may provide a basis for focal abnormalities as well. Several previous DTI studies in chronic schizophrenia showed decrease of FA in schizophrenics mainly in the front-temporal white matter and corpus callosum (Buchsbaum et al., 1998; Lim et al., 1999; Agartz et al., 2001; Burns et al., 2003). Furthermore, FA decrease in patients with first episode schizophrenia might be less pronounced compared to chronic patients (Price et al., 2005; Szeszko et al., 2005), suggesting that the decreased FA in schizophrenics might be attributed, at least in part, to progressive and exaggerated age-dependent changes in schizophrenics rather than neurodevelopmental abnormalities in the WM. To date, there is only one cross-sectional study with a small sample size investigating age-related FA changes in schizophrenia that demonstrated an age-related FA increase in schizophrenics (Jones et al., 2006).

The present study was aimed to examine whether patients with chronic schizophrenia do have reduced FA values compared to controls and whether such changes in FA progress in an age-dependent manner.

2. Methods

2.1. Subjects

Table 1 shows the characteristics of participants of this study. Forty-two patients with chronic schizophrenia were recruited at the National Center of Neurology and Psychiatry, Tokyo, Japan. Consensus diagnosis was made for each patient by at least two trained psychiatrists according to the DSM-IV criteria (American Psychiatric Association, 1994), based on all available information, including clinical interviews, medical records and other research assessments. All patients were stable and/or partially remitted and had been taking antipsychotic medication at the time of MR measurement and neuropsychological tests. Forty-two healthy volunteers who had no current or past contact to any psychiatric services served as controls. All the subjects were biologically unrelated Japanese. After description of the study, written informed consent was obtained from every subject. The study protocol was approved by the ethics committee of the National Center of Neurology and Psychiatry, Tokyo, Japan. Exclusion criteria for all the participants included asymptomatic or symptomatic cerebral infarctions detected by T2 weighted MRI, serious neurological or endocrine disorder, any medical condition that could potentially affect the central nervous system, or mental retardation according to DSM-IV criteria.

2.2. Image acquisition

MR studies were performed on a 1.5 tesla Magnetom Vision Plus system (Siemens, Erlangen, Germany). Axial DTI scans aligned to the plane containing anterior and posterior commissures were acquired with a pulsed-

Table 1
Characteristics of participants

	Controls	Schizophrenics	Two sample *t*-test	(Two-tailed; df=82)
			t	*P*
Number of subjects	42	42		
Gender (male/female)	26/16	26/16		
Handedness (right/left)	41/1	41/1		
Age (years)	39.2 (9.0)	40.0 (9.3)	−0.42	0.68
Range of age (years)	22–59	22–59		
Education (years)	17.1 (3.5)	13.0 (2.9)	8.1	<0.001
Full-scale IQ (WAIS-R)	114.3 (11.6)	86.0 (21.3)	6.0	<0.001
Age of onset		23.3 (7.0)		
Duration of illness (years)		16.8 (9.0)		
Duration of hospitalization (months)		31.2 (61.3)		
Dose of total antipsychotic drugs (mg/day, chlorpromazine equivalent)		1005.1 (735.3)		
Dose of typical antipsychotic drugs (mg/day, chlorpromazine equivalent)		694.8 (748.3)		
Dose of atypical antipsychotic drugs (mg/day, chlorpromazine equivalent)		310.3 (464.2)		

Mean (S.D.).
WAIS-R: Wechsler Adult Intelligence Scale-Revised.

gradient, spin-echo, single-shot echo planar imaging (EPI) sequence (TR/TE=4000/100 ms; acquisition matrix, 256×256; NEX=4, FOV 240 mm; b=1000 s/mm^2; 20 slices, slice thickness 5 mm, gap 1.5 mm). Diffusion was measured along six non-collinear directions. For each of six gradient directions, four acquisitions were averaged. Four acquisitions without diffusion weighting (b=0) were also averaged. Additionally, a three dimensional volumetric acquisition of a T1-weighted gradient echo sequence with a gapless series of thin sagittal sections using an MPRage sequence (TR/TE=11.4/4.4 ms; flip angle, 15 degree; acquisition matrix, 256×256; NEX=1, FOV 315 mm; slice thickness 1.23 mm) was acquired for evaluating the volume of grey matter (GM), WM and cerebrospinal fluid (CSF) space.

2.3. Image processing

FA images for each subject were computed from seven diffusion images acquired as above by an in-house script on Matlab 6.5 software (Mathworks, Inc., MA, USA). Then, the FA images were spatially-normalized using high-dimensional-warping algorithm (Ashburner et al., 1999) and were matched to the FA template image. To make the FA template image, we warped FA images of 4 normal subjects (other than 42 control subjects) to the single-subject T1 template (skull stripped image) using spatial normalization function of SPM2 and averaged the 4 warped FA images. The transformed FA images were smoothed with a Gaussian kernel. The filter size (full-width at half-maximum: FWHM) was varied from zero to 16 mm in steps of 2 mm to validate the consistency of results of SPM analyses, because a previous study (Jones et al., 2005) reported that the statistical results of SPM analyses were differed depending on filter size. For measuring the volume of GM, WM and CSF space, an additional function of an optimized VBM script (http://dbm.neuro.uni-jena.de/vbm) was used (Good et al., 2001).

2.4. Statistical analysis

2.4.1. Voxel-by-voxel analysis

The resultant FA images were analyzed using statistical parametric mapping with the framework of the General Linear Model in SPM2 (Wellcome Department of Cognitive Neurology, London, UK) (Friston et al., 1995). We constituted following three

Table 2
The relationship between smoothing kernel sizes (FWHM) and number of resels in our sample

FWHM (mm)	Number of resels
None	12460.4
2×2×2	5131.1
4×4×4	1720.2
6×6×6	706.0
8×8×8	289.4
10×10×10	119.7
12×12×12	52.1
14×14×14	24.4
16×16×16	12.4

statistical analyses: 1) a two-sample *t*-test for estimating group differences (controls versus schizophrenics), 2) a correlational analysis between age and FA values in both controls and the schizophrenics and 3) a correlational analysis of FA values with duration of illness, age of onset, duration of hospitalization, and daily dose of

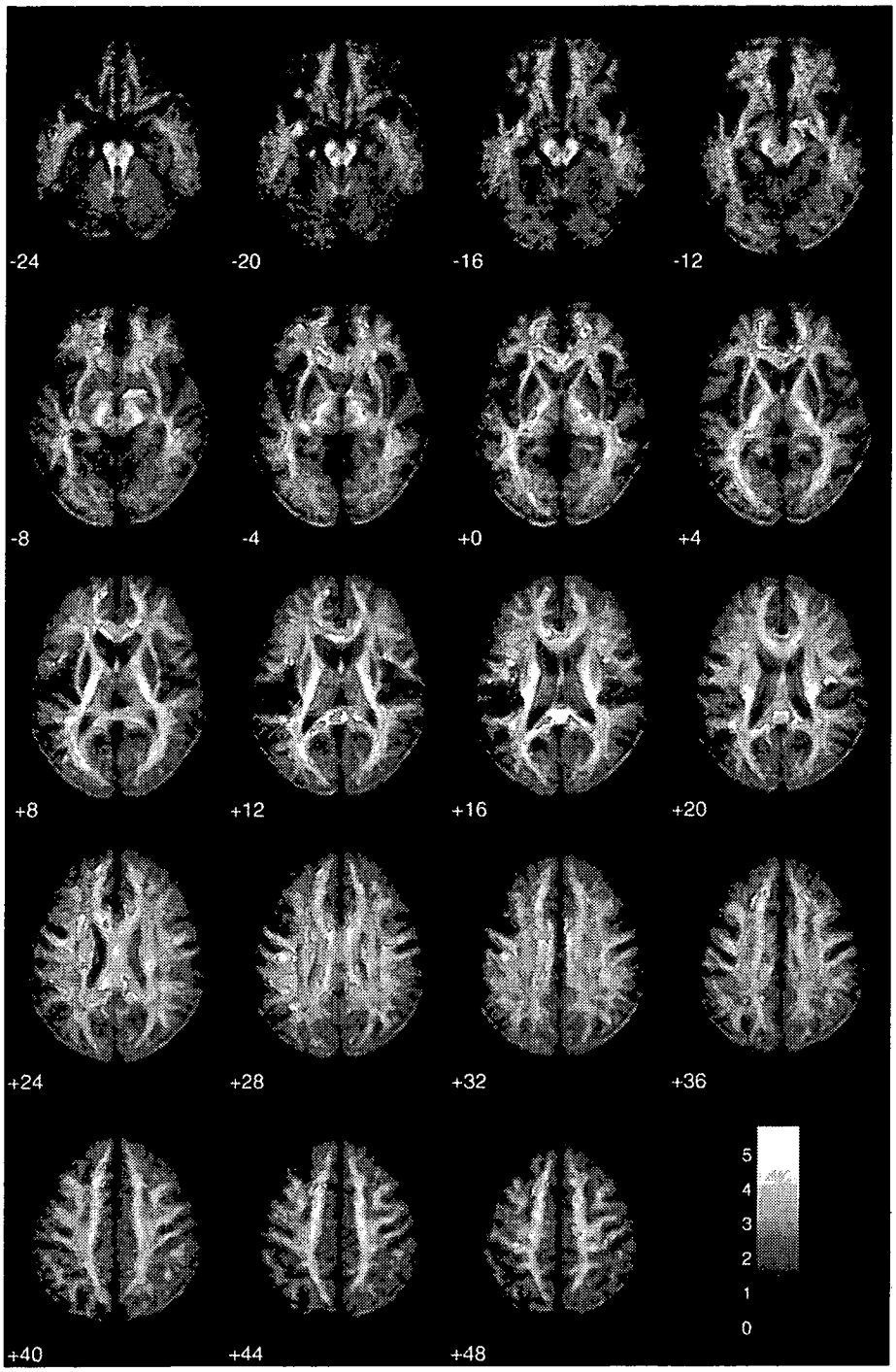

Fig. 1. Comparison in FA values between patients with schizophrenia and controls. The SPM {t} is displayed onto axial FA template images. The WM areas in which significantly lower FA values in patients compared with controls were observed, including the bilateral frontal and temporal WM, uncinate fasciculi, cingulum bundles, and genu and splenium of the corpus callosum ($P<0.001$, uncorrected).

antipsychotic drugs in the schizophrenics. In all the three analyses, relative WM volume (WM volume divided by the summation of GM, WM and CSF volumes) and WAIS-R (Wechsler Adult Intelligence Scale-Revised) full-scale IQ score were treated as nuisance variables. The former was included for eliminating the possible effect of WM volume change associated with aging on the FA values through partial voluming from non-WM voxels. The latter was included to allow for the effects of IQ, because there was some evidence which suggested DTI measures were correlated with cognitive decline in elderly (O'Sullivan et al., 2004). We additionally conducted the analyses without these two nuisance variables to check whether there were any differences in the results with or without nuisance variables in the statistical models. To estimate population effects (diagnostic effects), we used a single-subject, condition (controls or schizophrenics) and covariate (no covariate of interest) model for the SPM analysis. In the second analysis, we applied the single subject condition (controls or schizophrenics) and covariate (interaction with condition, covariate of interest; age) model. A single-subject, covariate only model was applied in the third analysis. For these three analyses, we set masking threshold for FA values of 0.2 for excluding voxels containing partial volume of WM and other tissues. Since the previous study demonstrating a positive correlation between FA values and age in schizophrenics reported mean FA values of around 0.4 (Jones et al., 2006), we additionally set masking threshold for FA values of 0.35 for examining correlation between age and FA values of more anisotropic WM structure in the second analysis. For the evaluation of the statistical models, we used Wake Forest University Pickatlas (Maldjian et al., 2003) to pick up cerebral WM in the Montreal Neurological Institute (MNI) space. We used uncorrected $P<0.001$ as a statistical threshold to search significant differences. As demonstrated in Table 2, the number of resels differed profoundly depending on smoothing kernel sizes (FWHM) and the statistical results with correction for multiple comparisons could change dramatically relying on number of resels. On the other hand, SPM results without correction for multiple comparisons were essentially unchanged regardless of smoothing kernel size (data not shown). Therefore, we did not perform correction for multiple comparisons. The resultant set of t values constituted statistical parametric map (SPM {t}). We employed the filter size of 6 mm for presentation of the results considering for the original voxel dimensions of acquired data {0.94 mm × 0.94 mm × (5.00+1.50) mm}.

2.4.2. ROI analysis

To ensure the robustness of the results of the voxel-by-voxel analyses, we additionally performed ROI analyses. We used MarsBar (http://marsbar.sourceforge.net/) for extracting region of interest (ROI) containing all the voxels classified as WM with Wake Forest University Pickatlas from spatially normalized and smoothed FA images and calculated mean FA values of the ROI. Then, we performed correlational analyses of mean FA values with the same variables in voxel-by-voxel analysis using Statistical Package for Social Science (SPSS), 1) in both controls and schizophrenics, 2) in controls and 3) in schizophrenics. We constituted a General Linear Model for the first analysis and entered diagnosis-by-age interaction effects into the statistical model to examine if there were any diagnosis-by-age interaction effects. For the second and third analyses, Pearson's correlation coefficients between mean WM FA values and covariates were calculated.

3. Results

3.1. Voxel-by-voxel analyses

3.1.1. Comparison between schizophrenics and controls

Schizophrenics demonstrated significantly lower FA values in widespread WM areas, compared with controls. These WM areas included bilateral frontal and temporal lobes, uncinate fasciculi (external capsules), cingulum bundles, and genu and splenium of corpus

Table 3
The summary of the WM areas in which significantly lower FA values in patients compared with controls were observed

Anatomical regions	*t*-value	MNI coordinates		
	(Voxel level)	*x*	y	z
Rt frontal lobe white matter	4.34	22.5	52.5	−4.5
Lt frontal lobe white matter	5.43	−13.5	49.5	−6
Rt temporal lobe white matter	4.25	48	−33	−7.5
Lt temporal lobe white matter	4.19	−45	−31.5	−10.5
Rt uncinate fasciculus (external capsule)	4.00	33	12	−1.5
Lt uncinate fasciculus (external capsule)	3.84	−33	12	−1.5
Rt cingulate bundle	4.23	6	6	33
Lt cingulate bundle	4.32	−7.5	6	30
genu of corpus callosum	3.79	6	24	10.5
splenium of corpus callosum	4.18	−3	−33	19.5

callosum (Fig. 1, Table 3). There would be increased possibility of alpha errors because we did not perform correction for multiple comparisons. However, our results were in well concordance with the results of the previous studies (Buchsbaum et al., 1998; Lim et al., 1999; Agartz et al., 2001; Burns et al., 2003; Kubicki

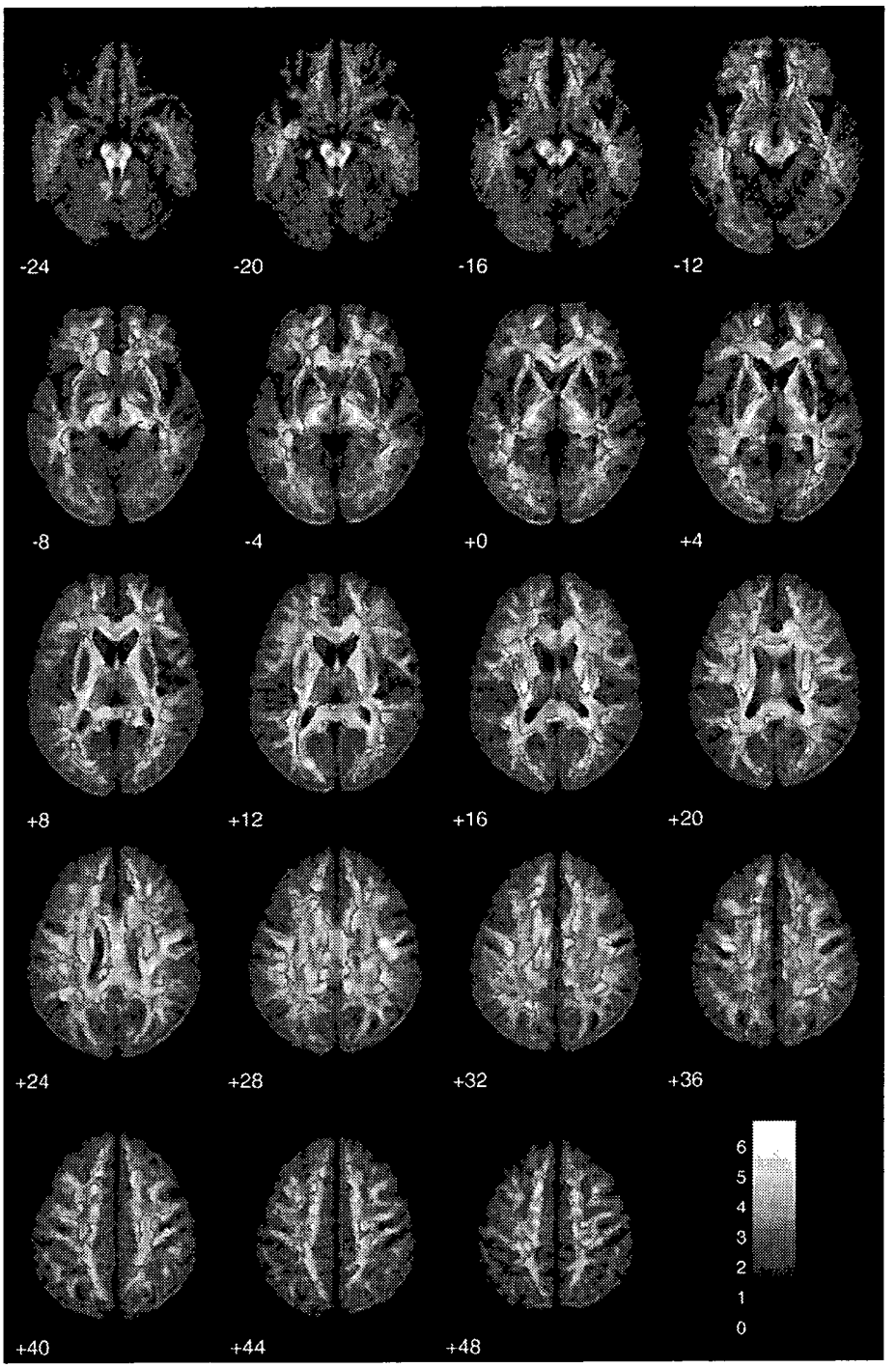

Fig. 2. Correlational analysis between FA values and age with 0.2 as a masking threshold in schizophrenics. The SPM {t} is displayed onto axial FA template images. The widespread WM areas showed a significant negative correlation between FA values and age in schizophrenics ($P<0.001$, uncorrected).

et al., 2003). Therefore, we might be able to regard the results of these previous studies as a priori hypotheses. There were no areas of significantly higher FA values in patients compared with controls even at a lenient threshold ($P<0.05$, uncorrected). In these results of the analysis without nuisance variables in the statistical

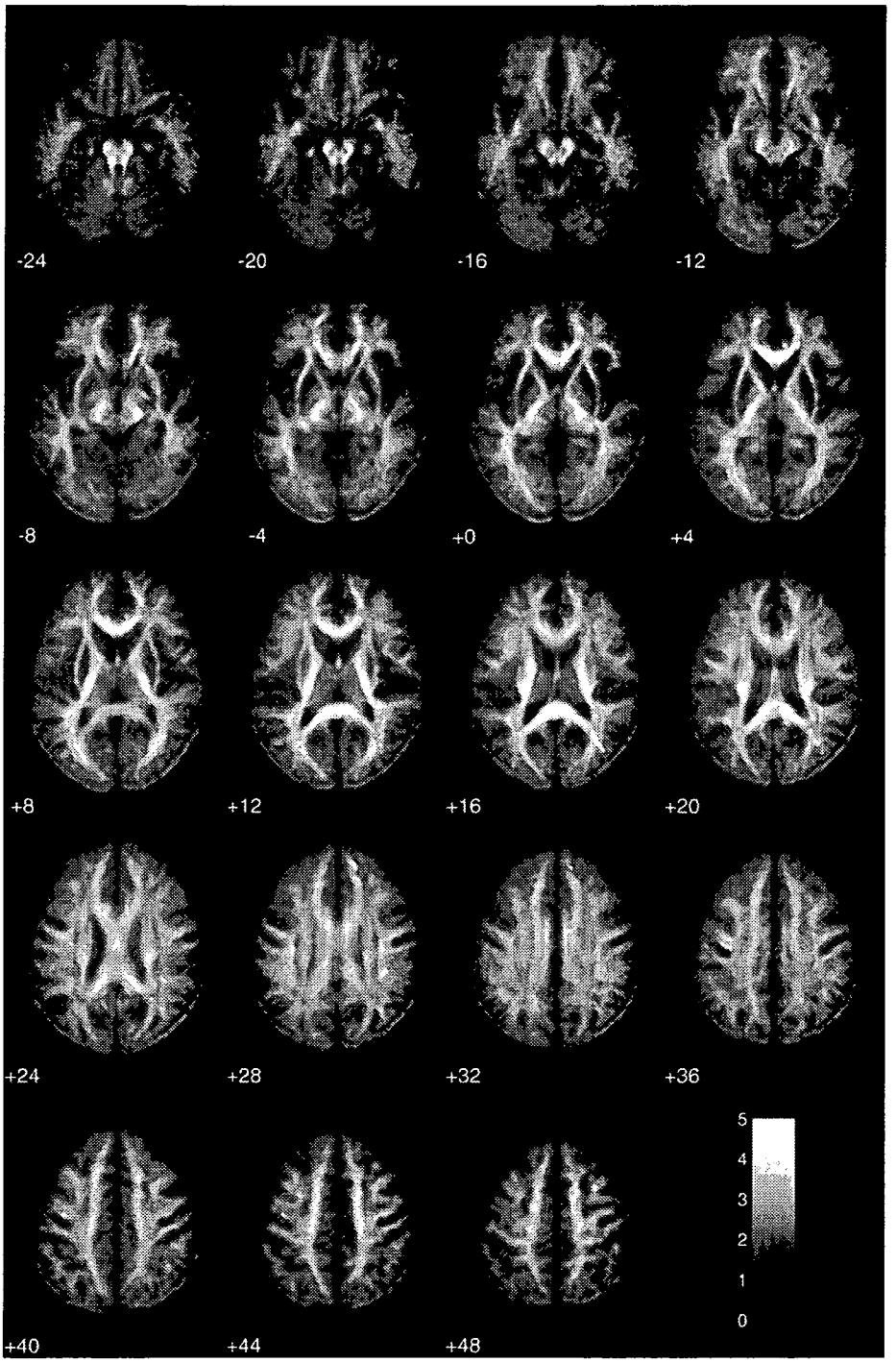

Fig. 3. Correlational analysis between FA values and age with 0.2 as a masking threshold in controls. The SPM {t} is displayed onto axial FA template images. The WM areas showed a significant negative correlation between FA values and age in controls ($P<0.001$, uncorrected), including right prefrontal {(15.0, 49.5, 30.0) in MNI coordinates, $t=5.03$}, left frontal {(−37.5, −15.0, 34.5), $t=4.51$} and bilateral temporo-occipital WM {(31.5, −60.0, 16.5), $t=4.75$; (−30.0, −60.0, 15.0), $t=4.47$}.

models, the distributions of the statistically significant areas were essentially unchanged compared to the results with nuisance variables although the spatial extents of the statistically significant areas were slightly larger (data not shown), which was the case with the results of other two analyses.

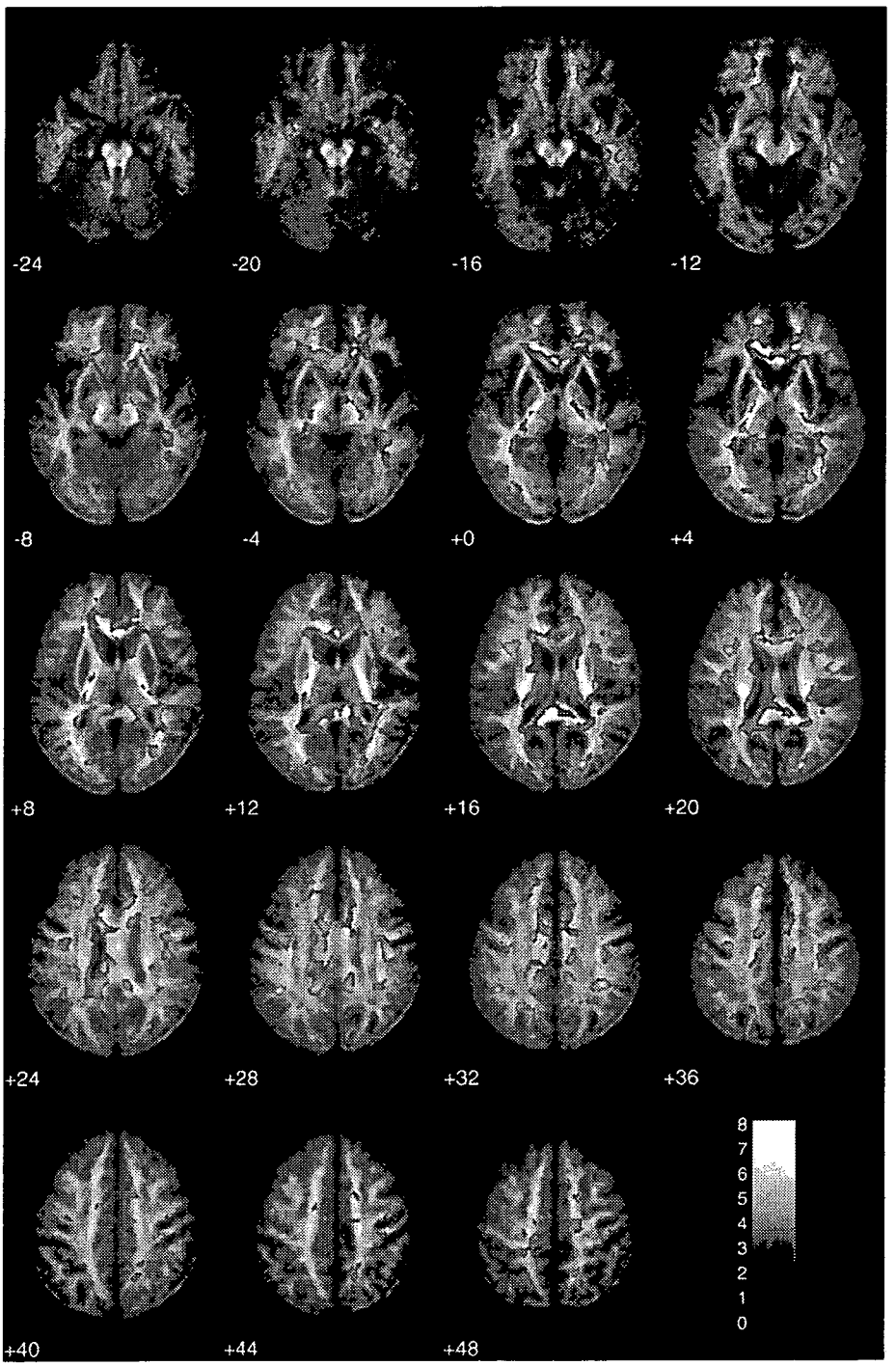

Fig. 4. Correlational analysis between FA values and duration of illness with 0.2 as a masking threshold in schizophrenics. The SPM {t} is displayed onto axial FA template images. The widespread WM areas showed a significant negative correlation between FA values and duration of illness in schizophrenics ($P<0.001$, uncorrected).

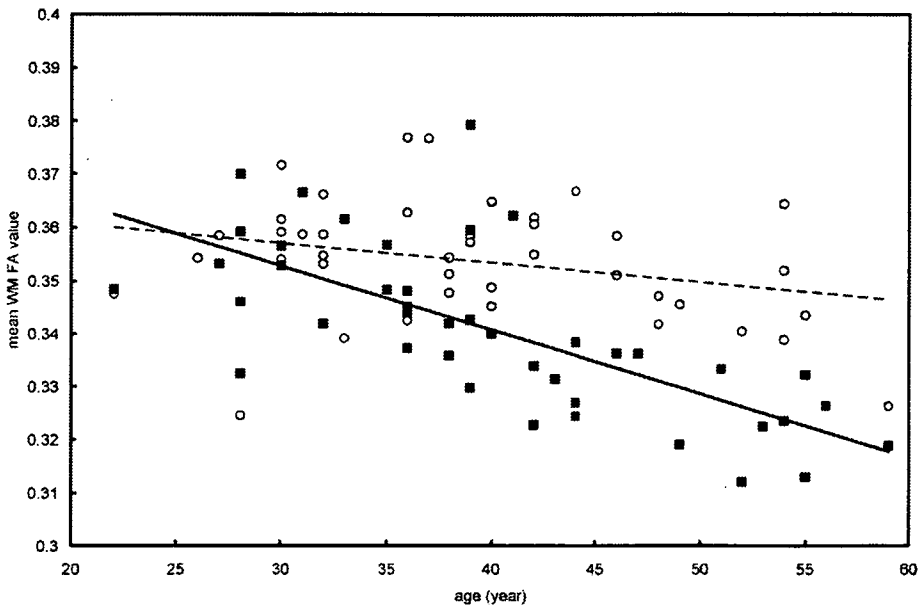

Fig. 5. A scatter plot between age and mean WM FA value when masking threshold for FA values was set to 0.2. Filled squares represent schizophrenics and open circles represent controls. The solid line indicates a regression line for schizophrenics ($y=-0.0012\times+0.3888$, $R^2=0.49$, test for regression slope: df=40; $t=-6.24$; $P<0.0001$). The dashed line indicates a regression line for controls ($y=-0.0004\times+0.3679$, $R^2=0.083$, test f or regression slope: df=40; $t=-1.90$; $P=0.065$). A significant diagnosis-by-age interaction effect (general linear model: $P=0.009$) was noted.

3.1.2. Correlational analysis in schizophrenic and control groups

As the results of the second analysis considering aging effects, a significant negative correlation with age was observed in the FA values of widespread, almost diffuse WM areas in the schizophrenic group (Fig. 2), while in the control group, only FA values in right prefrontal {(15.0, 49.5, 30.0) in MNI coordinates, $t=5.03$}, left frontal {(−37.5, −15.0, 34.5), $t=4.51$} and bilateral temporo-occipital WM {(31.5, −60.0, 16.5), $t=4.75$;

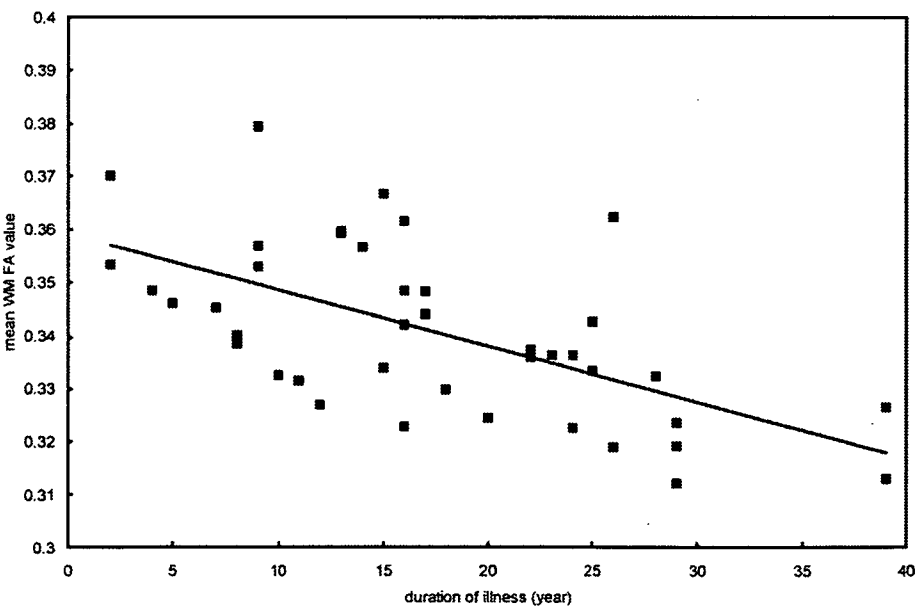

Fig. 6. A scatter plot between duration of illness and mean WM FA value when masking threshold for FA values was set to 0.2. Filled squares represent schizophrenics. The solid line indicates a regression line for schizophrenics ($y=-0.0011\times+0.3590$, $R^2=0.36$, test for regression slope: df=40; $t=-4.78$; $P<0.0001$).